Markus Hackl, BSc

# Reactive Separation of Acetic Acid with Supported Liquid Membrane Permeation Equipment

**MASTER'S THESIS**

to achieve the university degree of

Diplom-Ingenieur

Master's degree programme: Chemical and Pharmaceutical Engineering

submitted to

**Graz University of Technology**

Supervisor

Ass.Prof. Dipl.-Ing. Dr.techn. Marlene Kienberger

Institute of Chemical Engineering and Environmental Technology

Graz, January 2017

# Danksagung

An dieser Stelle möchte ich mich bei allen bedanken, die mich bei der Erstellung dieser Arbeit unterstützt haben.

Ein herzlicher Dank geht an Herr Professor Matthäus Siebenhofer, der es mir ermöglicht hat, diese Arbeit am Institut für Chemische Verfahrenstechnik und Umwelttechnik durchzuführen. Ein besonderer Dank gilt Frau Dr. Marlene Kienberger für die exzellente fachliche Betreuung meiner Diplomarbeit und die vielen konstruktiven Gespräche im Zuge dieser Arbeit. Dem Laborteam des Instituts unter der Leitung von Frau Ing. Herta Luttenberger danke ich für die Unterstützung während der Versuche und angenehme und freundliche Arbeitsatmosphäre.

Ganz herzlich möchte ich mich bei meiner Familie bedanken. Ein aufrichtiger Dank gilt meinen Eltern Fritz und Elisabeth, die mich in jeder Lebenssituation unterstützen. Durch ihre Hilfe und Rückhalt war es mir erst möglich, diese Ausbildung zu erreichen. Danke!

Deutsche Fassung:

Beschluss der Curricula-Kommission für Bachelor-, Master- und Diplomstudien vom 10.11.2008

Genehmigung des Senates am 1.12.2008

# EIDESSTATTLICHE ERKLÄRUNG

Ich erkläre an Eides statt, dass ich die vorliegende Arbeit selbstständig verfasst, andere als die angegebenen Quellen/Hilfsmittel nicht benutzt, und die den benutzten Quellen wörtlich und inhaltlich entnommenen Stellen als solche kenntlich gemacht habe.

Graz, am 12.01.2017 ……

(Unterschrift)

Englische Fassung:

# STATUTORY DECLARATION

I declare that I have authored this thesis independently, that I have not used other than the declared sources / resources, and that I have explicitly marked all material which has been quoted either literally or by content from the used sources.

Graz, 12.01.2017 ……

date (signature)

# Kurzfassung

Die Abtrennung von in Abwasserströmen enthaltenen Carbon- und Hydroxycarbonsäuren gewinnt immer mehr an Bedeutung. Insbesondere Abwasserströme aus der Papier- und Zellstoffindustrie sind dabei aufgrund des hohen Aufkommens von Interesse und Membranprozesse werden auf ihre Anwendbarkeit zur Abtrennung dieser organischen Säuren erforscht.

Diese Arbeit untersucht die Anwendbarkeit eines Membranreaktors mit gestützter Flüssigmembran zur Abtrennung von organischen Säuren aus wässrigen Lösungen. Als Modellkomponente wurde Essigsäure gewählt; die organische Phase bestand aus *n*-Octanol verdünnt in *n*-Undecan.

Im ersten Teil der Arbeit wurde die Veresterung in der organischen Phase mit den Katalysatoren Amberlyst® 15 und *4*- Dodecylbenzensulfonsäure untersucht. Mit beiden Katalysatoren werden Essigsäureumsätze > 82 % erzielt. Der zweite Teil der Arbeit kombiniert die Extraktion und Veresterung unter der Verwendung von Amberlyst® 15, *4*- Dodecylbenzensulfonsäure und Schwefelsäure als Katalysatoren. Bei einem Phasenverhältnis von 1:1 (v/v) und 50°C führt *4*- Dodecylbenzensulfonsäure schon bei einer Konzentration von 0.1 w% bezogen auf die organische Phase, zur Bildung stabiler Emulsionen. Amberlyst® 15 und Schwefelsäure führen aufgrund einer geringen Essigsäurekonzentration in der organischen Phase, im direkten Zweiphasenkontakt zu einem Umsatz von < 1 %. Um die Essigsäurekonzentration in der organischen Phase zu erhöhen, wurde Trioctylamin als Reaktivextraktionsmittel zugesetzt und der Einfluss auf die Veresterung mit Amberlyst® 15 untersucht. Die Zugabe von Trioctylamin verringerte den Umsatz der Essigsäure durch dessen Wechselwirkungen mit dem Katalysator.

Im letzten Teil der Arbeit wurden Extraktion und Veresterung im Membranreaktor kombiniert und zwei Vorgehensweisen näher untersucht. Die erste Methode verwendete *4*- Dodecylbenzensulfonsäure als Katalysator in Hinblick auf die Emulsionsvermeidung im Zweiphasenkontakt. Die Emulsionsbildung konnte bei Katalysatorkonzentrationen < 1 w% vermieden werden. Dabei wurden 17.3 ± 0.6 % der Essigsäure innerhalb von 24 Stunden bei 20°C umgesetzt. Im zweiten Ansatz wurde die physikalische Extraktion der Essigsäure mit der Veresterung in der organischen Phase durch Amberlyst® 15 kombiniert. Mit steigender Temperatur und Essigsäurekonzentration steigt der Stoffstrom durch die Membran, der dabei sinkende Umsatz bei 2 w% Amberlyst® 15 deuten auf eine Diffusionslimitierung im Katalysator hin. Für eine Essigsäurekonzentration von 60 g/L in der wässrigen Phase wurde ein Umsatz von 2.7 ± 0.4 % innerhalb von 24 Stunden bei 50°C erreicht.

# Abstract

The removal of carboxylic and hydroxycarboxylic acids from aqueous effluents is gaining in importance. Due to their large amounts, effluents of the pulp and paper industry are of interest, and membrane based processes are studied for the removal of these organic acids.

This work investigated the applicability of a supported liquid membrane reactor for the removal of low concentrated organic acids from aqueous effluents. Acetic acid was chosen as the model compound, the organic phase consisted of *n*-octanol diluted in *n*-undecane.

The first part of this work studied the esterification in the organic phase, using Amberlyst® 15 and *4*- dodecylbenzenesulfonic acid as catalysts. With both catalysts, an acetic acid conversion of > 82 % was achieved. The second part combined the extraction and esterification using Amberlyst® 15, *4*- dodecylbenzenesulfonic acid and sulfuric acid as catalysts. At a phase ratio of 1:1 (v/v) and 50°C, *4*- dodecylbenzenesulfonic acid leads to the formation of a stable emulsion, even at DBSA concentration of 0.1 w% with respect to the organic phase. Amberlyst® 15 as well as sulfuric acid showed a conversion of acetic acid of < 1 % due to the low concentration of acetic acid in the organic phase. To increase the acetic acid concentration in the organic phase, trioctylamine was added and the influence on the esterification was studied. The addition of trioctylamine reduced the conversion of acetic acid due to interaction with the catalyst.

The last part of the work combined extraction and esterification in a membrane reactor, two different approaches were investigated. The first approach used *4*- dodecylbenzenesulfonic acid as catalyst to avoid emulsification of the two- phase system. Emulsion formation was prevented at catalyst concentrations < 1 w% and a conversion of acetic acid in the feed phase of 17.3 ± 0.6 % within 24 hours at 20°C was achieved. The second approach combined the physical extraction of the acid with subsequent esterification in the organic phase using Amberlyst® 15. With increasing temperature and acetic acid concentration in the feed phase, the conversion at 2 w% Amberlyst® 15 declined, indicating diffusion limitation in the used catalyst. For a representative acetic acid concentration of 60 g/L, a conversion of 2.7 ± 0.4 % within 24 hours at 50°C was obtained.

# Table of Content

# 1 Introduction

Low molecular weight carboxylic and hydroxycarboxylic acids such as formic acid, acetic acid and lactic acid are widely used organic bulk substances. Formic acid and derivatives are mainly found in leather and textile industry and animal feed preparation whereas acetic acid and acetate esters are primarily used as solvents [1], [2]. Both acetic acid and lactic acid find main employment in polymer industry, lactic acid and derivatives are further used in food industry [2], [3].

Black liquor from the pulping process contains considerable amounts of low molecular weight organic acids [4], [5]. The corrosive properties of the acids, regulatory bodies and the fact that they can be used for further synthesis to obtain value-added products, lead to a high interest for efficient and economic extraction of the acids from waste water streams [2].

Many approaches for the recovery of carboxylic acids from aqueous waste stream exist. Reactive distillation and extraction are widely applied industrial methods, but other technologies such as reactive chromatography and reactive extraction are studied for industrial applicability [6]–[10]. Each method is designed for a certain operation range, the reactive distillation is economically applicable, if the concentration of the acid is > 30 w% [6], [7], [11]. For lower acid concentrations, reactive extraction is of interest, but extraction efficiency decreases with decreasing acid concentration [10], [12]. Membrane based processes are studied for the removal of low concentrated organic acids [13], [14] in combination with a chemical reaction in the receiving phase [15]. High effective catalysts for a two phase esterification reaction, such as *4*- dodecylbenzenesulfonic acid, suffer from the drawback of emulsification in stirred direct-phase contact [16]–[18]. Emulsions can be separated by gravity or centrifugal forces, by chemical demulsifiers and external fields such as temperature, ultrasound or electrostatic field [19], [20], [21]. A phase separation can also be achieved by filtration over tailored membranes [22].

This work investigates the applicability of a supported liquid membrane extraction in combination with esterification as a method for the removal of carboxylic and hydroxycarboxylic acids from dilute systems using acetic acid as a model compound. The removal of acetic acid from the aqueous phase is studied using *4*- dodecylbenzenesulfonic acid as catalyst under the aspect of emulsion avoidance with a rigid membrane in cross current operation. In addition, the physical extraction of acetic acid through the supported liquid membrane with subsequent esterification in the receiving phase is studied.

# 2 Theoretical Background

## 2.1 Esterification and Deep Eutectic Solvents

Esterification terms the reaction of a carboxylic acid with an alcohol. The products of this reaction are the ester and water. Fig. 2-1 illustrates the reaction of acetic acid with octanol to produce octyl acetate and water.

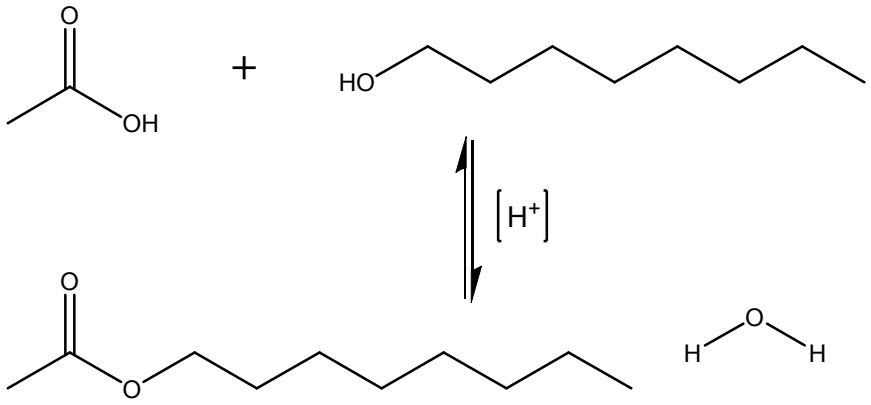


Fig. 2-1: Esterification of acetic acid with *n*- octanol

The esterification is an acid catalyzed equilibrium reaction in which the acid itself can act as a Brøwnsted acid catalyst but autocatalysis leads to low reaction rates and yields. Higher yields are possible at elevated temperatures [23].

In the presence of an additional catalyst, the esterification reaction proceeds much faster due to a decrease in activation energy [24]. The most commonly applied esterification reactions follow the Fischer or acid catalyzed mechanism. The first step involves the protonation of the carboxylic acid by a Brøwnsted acid, such as sulfuric acid. The protonated carbonyl carbon is then attacked by the nucleophilic alcohol to form a tetrahedral intermediate. The proton of the alcohol is transferred to one of the OH- groups of the former carbonyl carbon and lead to a more stable intermediate. Subsequently, the formed oxonium is eliminated as water to leave a protonated ester. In the final step, the proton is removed to result in the ester and regenerated catalyst. [25], [26].

An alternative reaction mechanism is proposed using heterogeneous catalysts, such as sulfonic acid immobilized on silica gel. Based on density functional theory (DFT) methods it is concluded that no proton transfer occurs, but the catalyst activates the substrates by formation of hydrogen bonds [27]. A study using propylsulfonic acid- functionalized mesoporous silica,

showed that both acetic acid and methanol adsorb at the catalyst and the esterification follows a dual- site Langmuir- Hinshelwood reaction mechanism in *1,4*- dioxane as solvent [28]. In contrast, a single- site Eley- Rideal mechanism is observed for Nafion®/ silica nanocomposite catalyst in tetrahydrofuran for the same reactants and similar conditions [29], hence the support of the functional group plays a role in the adsorption mechanism [28].

Homogeneous acid catalysts for organic phases incorporate benzenesulfonic acids and are applied, for instance, for transesterification in biodiesel production [16]–[18]. The reaction rate increases with increasing substitution of the aromatic ring. A study on the reactivity of substituted benzenesulfonic acids for the production of fatty acid methyl esters showed that *4*- dodecylbenzenesulfonic acid (DBSA) shows the highest yield among all investigated benzenesulfonic acids [18] with a $pK_A$ value of -1.8 [30]. Due to the long alkyl chain on the benzene sulfonic acid, DBSA remains preferably in the hydrophilic phase. In addition, DBSA acts as an anionic surfactant and creates emulsions which are difficult to separate by gravity [18]. The chemical structure of DBSA and the alignment at the phase interface is shown in Fig. 2-2 (left).

Deep eutectic solvents (DES) are mixtures of salts with a melting point below 100°C. The DES is formed by mixing a quaternary ammonium or metal salt with a hydrogen bond donor such as acids, amines or alcohols. Due to charge delocalization between the ammonium salt counter ion and hydrogen bond donor, the melting point is drastically decreased compared to the individual compounds. Compared to ionic liquids, many DES are prepared by readily accessible chemicals by a simple and safe one-step synthesis. DES feature low vapor pressure combined with a low melting point, but relatively high viscosity and density. They can be applied as a dual solvent- catalyst for a variety of organic transformations, including esterification [31], [32].

## 2.2 Emulsion Formation

Emulsions are classified as dispersed systems consisting of two immiscible liquids in which one liquid is dispersed in the other. The term dispersed phase refers to the dispersed liquid droplets which are surrounded by the continuous phase. Depending on the quantity ratio, the systems are classified as oil-in-water (O/W), water-in-oil (W/O) or oil-in-oil (O/O) emulsions, whereas the latter example is the result dispersing a polar oil in a non-polar oil or vice versa [33].

Molecules or atoms at the phase interface are exposed to an attraction force towards the bulk phase due to imbalanced atomic or molecular interactions. The surface tension ($\sigma_{surf}$) represents the force that is needed to compensate the attraction force of the molecules at the interface towards its bulk phase and defined is as force per unit length according to equation 2-1 [34]:

$$\sigma_{surf} = \frac{F_c}{l} \quad \left[\frac{N}{m}\right] \tag{2-1}$$

The free surface energy of a liquid ($\Delta G_{surf}$) is defined as the amount of energy needed to create new surface area according to equation 2-2 [34]:

$$\Delta G_{surf} = \frac{E_{in}}{A_{new}} \quad \left[\frac{J}{m^2}\right] \tag{2-2}$$

Surface tension and free surface energy show the same units as it can be seen by comparing the units of equation 2-1 and 2-2. The free surface energy is alternatively defined as the amount of energy needed to move an atom or molecule from the bulk phase to the phase interphase, hence the surface tends to contract and droplets are formed [34].

While the two immiscible liquids are mixed with each other due to mechanical energy input, new surface is created and one liquid is dispersed in the other. If the energy input is interrupted, the dispersed droplets will coalesce and both phases will separate [33]. In the presence of a third component, an emulsifier or surfactant, the dispersed droplets are stabilized and coalescence is weakened. Depending on the size of the dispersed droplets, volume fraction of the dispersed phase and refractive index between both phases, the emulsion appears translucent or opaque/ milky [33].

Surfactants and emulsifiers such as DBSA consist of a hydrophilic (e.g. $SO_3^-$) and a hydrophobic (e.g. alkyl chain) group. In a two-phase system, for example an O/W emulsion, the surfactant aligns along the phase interphase of the two immiscible liquids. The non-polar alkyl chain remains inside the oil droplet, whereas the hydrophilic group points into the continuous aqueous phase. The alignment of the emulsifier along the phase interphase leads to a decrease of the free surface energy and surface tension which results in an emulsification of the system [20], [33], [34].

Depending on the dispersed system, amount of emulsifier and process conditions such as energy input or temperature, the system can be classified either as macroemulsion or microemulsion [20], [33], [34]. Macroemulsions (droplet size > 50nm) are kinetically stable but not thermodynamically stable, which leads to a breakdown of the emulsion by coalescence, since $\Delta G_{surf}$ is positive [33]. In microemulsions (droplet size < 50nm) micelles are formed and such emulsions are considered as thermodynamically stable, which means that no coalescence will occur. This behavior depends on the amount of emulsifier in the system and is characterized by the critical micelle concentration (CMC) [34]. Due to the same orientation of the surfactants, the micelle droplets repel each other which leads to hindered coalescence of the dispersed phase, thus preventing successful phase separation [33], [35]. Fig. 2-2 (right) illustrates this phenomenon.

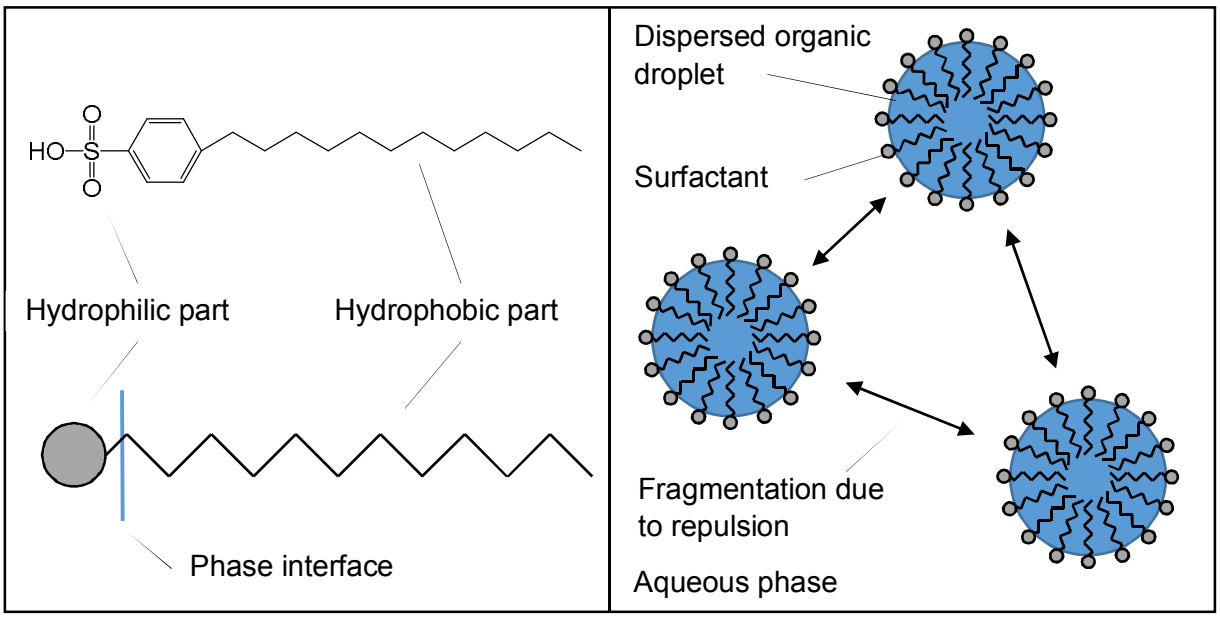


Fig. 2-2: Chemical structure of DBSA (top left), the alignment of a surfactant at the interface (bottom left) and repulsion of micelles (right). Modified from [35]

## 2.3 Liquid/ Liquid Extraction

During liquid/ liquid extraction, the solute is transferred from one liquid phase into the other phase. Requirements for a phase separation after contact is a density difference and immiscibility of both liquid phases.

A general flow chart of a physical liquid/ liquid extraction process is shown in Fig. 2-3 and comprises two steps, extraction and regeneration. The first step involves the direct phase contact of the feed phase loaded with the solute (either a valuable component or pollutant) and

regenerated solvent. At this step, the solute migrates from the feed phase into the solvent phase due to the concentration gradient and solubility in the solvent. The purified feed phase (raffinate) exits the extraction step and the enriched solvent phase (extract) is further treated to recover the solute and regenerate the solvent. The solvent regeneration can be implemented with any suitable separation process such as distillation or chemical stripping (re- extraction). After regeneration, the solvent is reused in the extraction step [36].

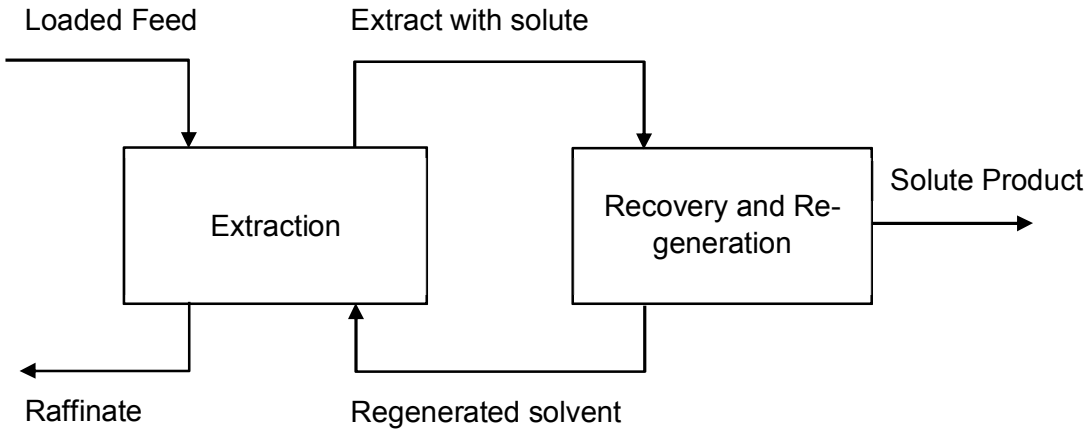


Fig. 2-3: General flow chart of an extraction process

In contrast to physical extraction, the solute undergoes a chemical reaction with an extracting agent in a reactive extraction process. The nature of the extracting agent depends on the compound which needs to be extracted. Metal cations are often extracted into an organic phase using aryl or alkyl substituted phosphoric acids such as di(2-ethylhexyl) phosphoric acid (D2EHPA). Anionic species such as deprotonated organic acids can react with a quaternary or ternary alkyl- substituted amine like trioctylamine (TOA). Quaternary ammonium salts are applicable for reactive extraction and can function as a phase transfer catalyst, which is described in section 2.1. The general flow chart depicted in Fig. 2-3 is valid for reactive extraction as well. Often, reactive extraction agents show high viscosity or occur as salts, hence a solvent, consisting of a reactive extraction agent, a modifier and diluent is utilized [37]. To regenerate the solvent and reactive extractive agent, the same unit operations as for physical extractions are used.

One important property of the solvent is the capacity for the solute. The capacity determines the solvent to feed ratio and depends on the distribution coefficient $K_{D\,i}$ which is defined in equation 2-3, [37].

$$K_{D\,i} = \frac{{c_i}^E}{{c_i}^R} \tag{2-3}$$

$c_i$ represents the concentration of substance $i$ in the raffinate ($R$) and extract phase ($E$). The larger $K_{D\,i}$, the higher the solubility of compound $i$ in the extract phase [37]. The solubility of a substance in the solvent can be enhanced by modifiers and reactive extraction agents. Modifiers such as aliphatic alcohols increases the solubility of carboxylic acids in a nonpolar solvent for physical extraction and also stabilize the solute- reactive extraction agent- complex in reactive extraction [38]–[40].

## 2.4 Concept of Liquid Membranes

A membrane is a semipermeable layer which separates two phases and usually consists of a solid polymer or an inorganic framework. A separation of different components is achieved if one substance diffuses faster through the membrane than the other components. In liquid membranes the semipermeable barrier consists of a liquid which is immiscible with the two phases that need to be separated [41], [42]. One advantage of liquid membranes over polymer membranes is the fact that diffusion in liquids is orders of magnitude higher than in polymers which results in larger fluxes through the liquid membrane [41].

Depending on the module design configurations, liquid membranes are classified into three categories [41], [42]:

1) Bulk Liquid Membranes (BLM)

In BLM, the feed and receiving phase are separated by a bulk membrane phase. The membrane phase is immiscible with the feed and receiving phase respectively and is usually supported with a polymeric layer.

2) Supported or Immobilized Liquid Membranes (SLM or ILM)

If the solid support layer is impregnated with the immiscible membrane phase, and hence the only barrier between feed and receiving phase, the system is classified as a supported liquid membrane.

3) Emulsion Liquid Membranes (ELM)

ELM are not supported by solid structures, instead the membrane phase is formed by dispersing the receiving phase into the (immiscible) membrane liquid. In case that the liquid membrane is an organic phase, a W/O emulsion is the result. The emulsion then dispersed in the feed phase resulting in a core bubble encased by the liquid membrane in the feed solution. In ELM applications, conventional extraction equipment can be used

Fig. 2-4 illustrates the types of liquid membranes. Bulk liquid membranes show, in contrast to other LM configurations, the lowest amount of transferred substance due to the relative thick membrane layer and is mainly used for studying of transport mechanism [41]. ELM achieve better fluxes due to the high surface/ volume ratio available for mass transfer. The membrane stability is a crucial aspect for industrial implementation of liquid membranes. In ELM applications, the dispersed membrane must be stable enough to avoid the mixing of feed and receiving phase. For subsequent recovery of the receiving phase, the emulsion splitting is difficult and the major drawback of ELM. For SLM the leaching of membrane liquid and subsequent membrane break through is a problem and depends on interfacial tension and carrier interactions with feed or receiving phase [41], [43].

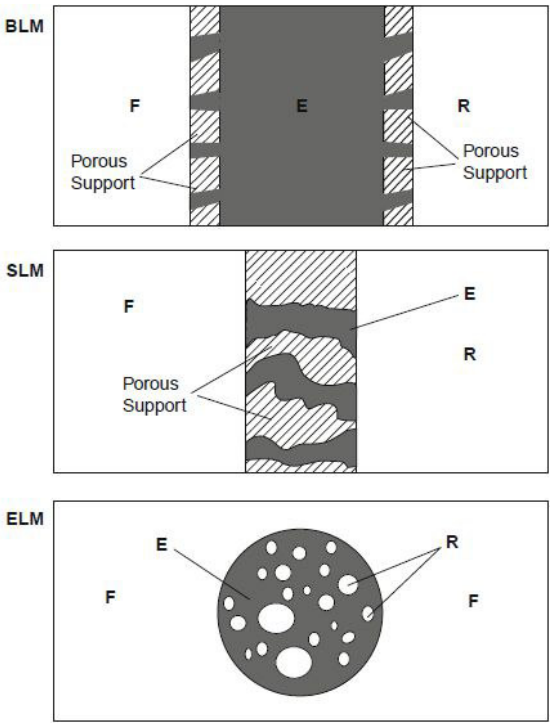


Fig. 2-4: Overview of liquid membrane configurations [19]. F: feed phase, R: receiving phase and E: liquid membrane phase.

## 2.5 Model Concept for the Esterification at the SLM Interface using DBSA

Based on the knowledge in esterification mechanism and liquid membrane permeation, the model concept for the esterification of acetic acid with *n*-octanol using DBSA as catalyst at the supported liquid membrane interface is developed.

Aqueous and organic bulk phase are separated by a rigid surface; the pores of the support layer are filled with organic phase. The aqueous phase consists of acetic acid in water and the organic phase is composed of *n*- octanol and DBSA in the aliphatic diluent *n*- undecane.

In the model concept illustrated in Fig. 2-5, both alcohol and catalyst diffuse through the membrane to the phase interface. Due to its surfactant properties, the catalyst aligns at the interface so that the polar sulfonic acid group is in the aqueous phase while the hydrophobic part of the molecule remains in the organic phase. The hydrophobic alcohol and acid undergo a hydrogen bond formation with the catalyst at the sulfonic acid group [27]. With both educts activated and bond at the catalyst, the esterification reaction proceeds. Due to the close location of reaction site at the interface, the resulting ester diffuses into the bulk of the organic phase while the side product water remains in the aqueous phase.

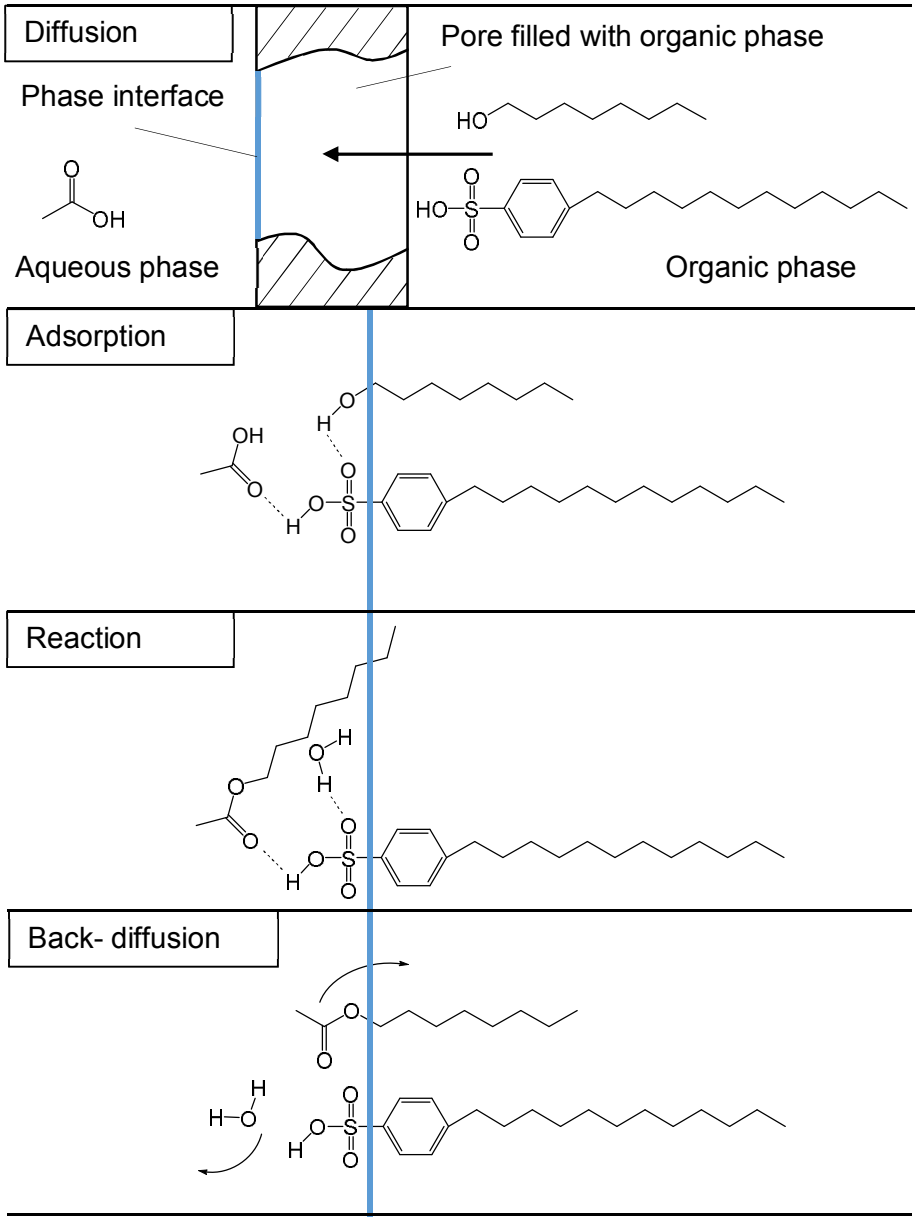


Fig. 2-5: Model concept for the esterification at the phase interface of organic and aqueous phase (blue line) using DBSA as catalyst

# 3 Experimental Setup

## 3.1 Batch Experiments

Batch experiments were performed in a 500 mL three-neck flask which was placed on a heat-on- block on a magnetic stirrer. The stirring speed was varied between 500 and 700 pm, depending on the used reaction matrix. The temperature was set to 50°C and controlled with a thermostat positioned in the reaction mixture. The experiments were performed at ambient pressure. To ensure constant conditions, a condenser was positioned on the flask and cooled with tap water. The assembly of the batch experiment setup is shown in Fig. 3-1.

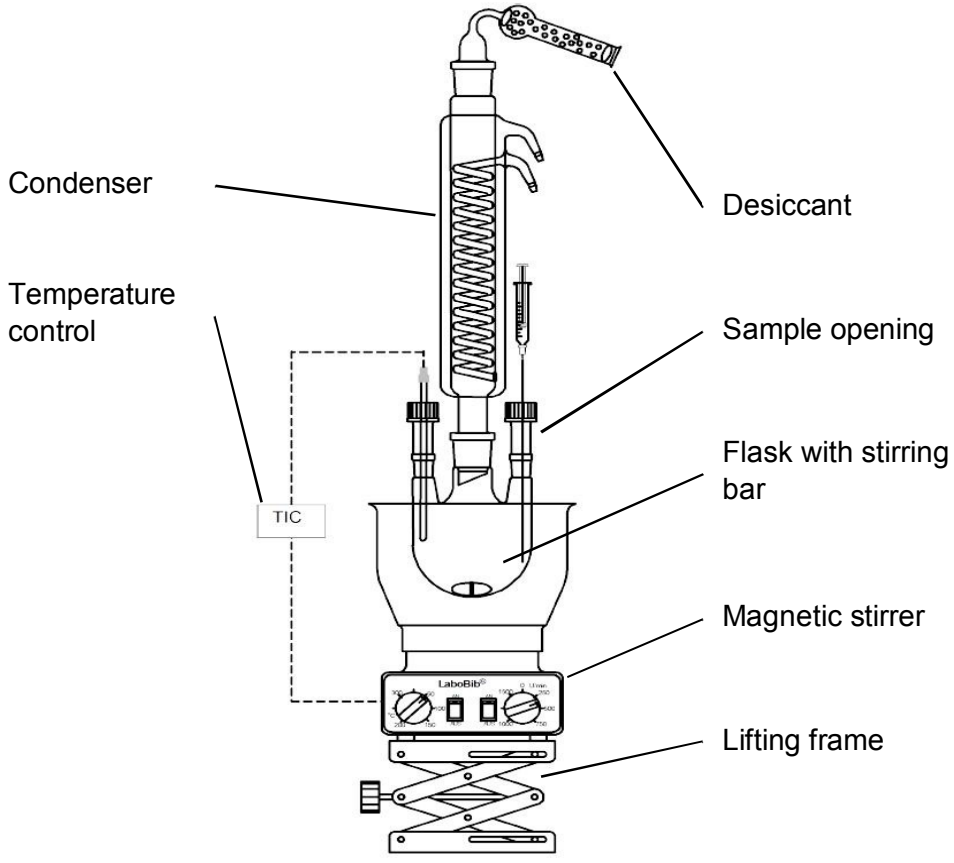


Fig. 3-1: Batch experiment setup

## 3.2 Reactor Designs and Start-up

Two different membrane reactors were used. The main focus in this work was on the small membrane reactor (25 cm² exchange area) due to temperature control and fast set-up. Supplementary experiments were performed using the larger membrane reactor (120 cm² exchange area). Due to the materials used for the production of the reactor, it is only possible to perform experiments at room temperature. Tab. 3-1 summarizes the specifications of the used membrane reactors.

Tab. 3-1: Comparison of membrane reactor specifications

| | Small | Large |
|---|---|---|
| Volume [mL] | 95; 215 | 108 |
| Membrane area [cm²] | 25 | 120 |
| Membrane material | PE | PE |
| Pore size range [µm] | 7-12 | 7-12 |
| Porosity [%] | 35 | 35 |

### 3.2.1 Small Membrane Reactor

The supported liquid membrane reactor is designed and build in a modular way. It consists of three main parts, two filling chambers for the organic and the aqueous phase, and the membrane module placed between the two filling chambers. All main parts are made of PVC-U. Each chamber includes one inlet and outlet with a connector for 8 mm tube or core thread with ¼ - 28 UNF. Depending on the size of the filling chamber, it is additionally equipped with two sight glasses opposite to each other. The membrane module itself consists of two membrane frames where the membrane sheet is glued in between, further the membrane module has 8 mm connectors for inlet and outlet. The membrane sheet is a commercially available porous polyethylene sheet with a pore size in the range of 7-12 µm and hydrophilic surface properties.

Fig. 3-2 shows two configurations of the membrane reactor. The left reactor is equipped with 215 mL filling chambers and sight glasses, the right configuration shows two membrane reactors, where each chamber holds 95 mL. Two different options for tube connections are shown on the 95 mL reactors. Setup A is equipped with 8 mm tube connectors (plugged); setup B is equipped with ¼ - 28 UNF core threads and connected to pump via male connectors.

The membrane module holds two dowel pins on each side to allow precise alignment of the filling chambers. The filling chambers and membrane module are joined together by five threaded rods. The type of sealing depends on the used solvents and is described in the following section.

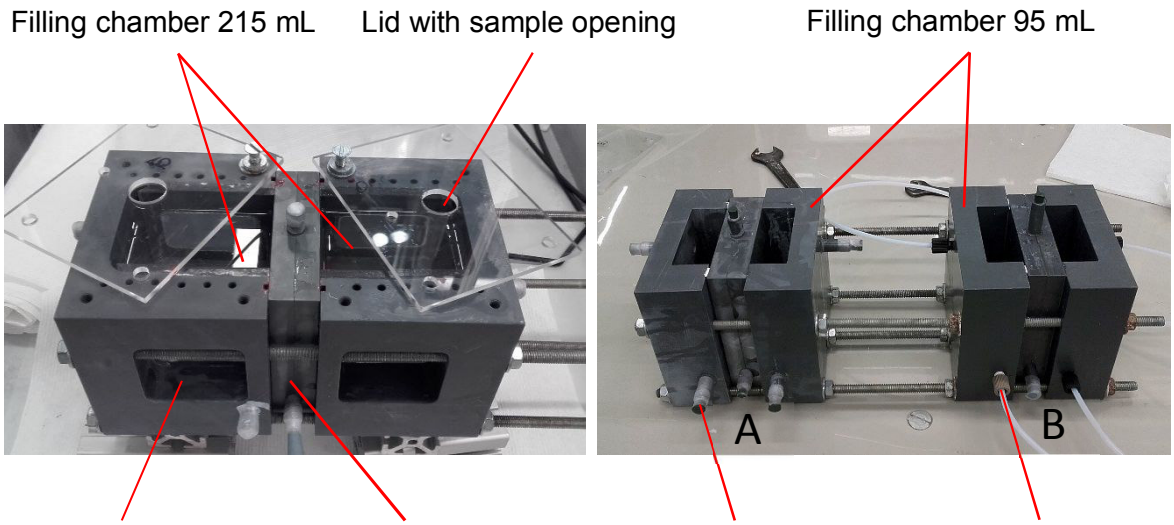


Fig. 3-2: Membrane reactor configurations. Left: 215 mL chambers with sight glasses and 8 mm tube connectors. Right: Two 95 mL modules with 8 mm tube connector (A) and ¼ - 28 UNF connector (B).

Assembly of the membrane reactor is done using three threaded rods. When the feed and receiving phase are aqueous phases, the sealing of the chambers against the membrane module was sufficient using standard caulking strips made of *Viton*®. When the receiving phase or both, receiving and liquid membrane phase were organic, leaking was observed after 24 hours. The organic media from the receiving phase penetrated the caulking strip and leaking of 1 % per hour, with respect to the filling chamber volume was noted. It was observed that the caulking strip was soaked with liquid and the latter was spread on top of the reactor surface as shown in Fig. 3-3 (left).

Instead of caulking strip, a flat sealing strip, which is used to seal gearboxes, was used but led to similar leaking as the caulking strip sealing. The material of the flat strip consists of densified *Viton*®; hence this material was not suitable for sealing the organic phase- filling chamber against the membrane module. To ensure an evenly distributed contact pressure along the sealing face, two additional threaded rods were implemented at each bottom corner of the filling chambers. The *Viton*® sealing was substituted by a fibrous PTFE flat sealing strip (*Klinger*® *Sealex*) which was one-sided sticking for easier attachment. The leaking of the organic phase was decreased compared to caulking strip sealing. Nevertheless, leaking was observed. Instead of solid sealing material, a pasty sealing agent (*Hylolite*® *Red 100*) was implemented subsequently. This paste kept its flexibility after the solvent (acetone) evaporated and fitted the surface of the membrane module and filling chamber. With this type of sealing applied, no leaking was recognized for the duration of the experiments (24 hours), however a dissolution of the sealing paste was observed at contact with organic phase as can be seen in Fig. 3-3 (right).

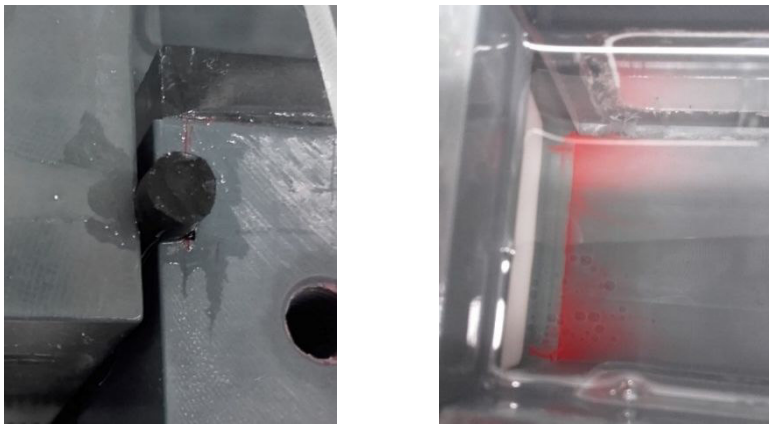

Fig. 3-3: Left: Detail view on caulking strip sealing and spreading of organic liquid. Right: Dissolution of sealing paste in organic phase

An appropriate solution to seal the membrane reactor was found in using compacted PTFE flat sealing strips (*Ammerflon*®). In contrast to the fibrous PTFE flat sealing, cavities inside the material were densified and resulted in a white- translucent appearance when pressure was applied. This sealing method allowed a flexible combination of different membrane modules and filling chambers and leaking was not observed during the experiments (24 hours). The sealing needed to be exchanged after dismantling the membrane reactor and the sealing strip was soaked with organic media, hence some leaking may appear after longer experimental times.

To permanently seal the organic filling chamber, it was glued to the membrane module using epoxy resin (*R&G Faserverbundwerkstoffe*®). This method has the drawback of difficult cleaning but represents a reliable method to seal the filling chamber for experiments which last several days. Tab. 3-2 summarizes the applicability of different sealing methods with respect to the media.

Tab. 3-2: Overview of applicable sealing methods depending on the used media

| Sealing method | Applicable for | |
|---|---|---|
| | Aqueous | Organic |
| Caulking strip- *Viton*® | Yes | No |
| Flat caulking strip- *Viton*® | Yes | No |
| Fibrous flat strip- PTFE | Yes | No |
| Sealing paste | Yes | No |
| Densified flat strip- PTFE | Yes | Yes* |
| Epoxy resin | Yes | Yes** |

* sealing needs to be renewed after each dismantling of membrane reactor

** permanently glued membrane module and filling chamber

The membrane exchange area for this type of reactor is identical for all configurations and is 25 cm². However, the modular design of the reactor allows to double the exchange area by using an additional filling chamber between two membrane modules. In this setup, the middle chamber contains the aqueous phase whereas the two outside chambers are filled with the organic phase. This reactor configuration is shown in Fig. 3-4.

Temperature control in the reactor is achieved by placing the reactor in a water bath, which is heated by a thermostat. In order to reach the desired temperature fast, the empty reactor and the prepared containers with reaction mixtures are preheated in the water bath.

Each filling chamber can be mixed individually by circulating the media through a peristaltic pump. The inlet to the filling chamber is located close to the membrane and parallel to the exchange area whereas the outlet is positioned opposite to the membrane. In addition, the fluid is pumped through a preheating coil, which is submerged in the water bath, prior to the inlet. The tubing material consists of PTFE or *Tygon*® *F-4040* and is resistant to the used fluids.

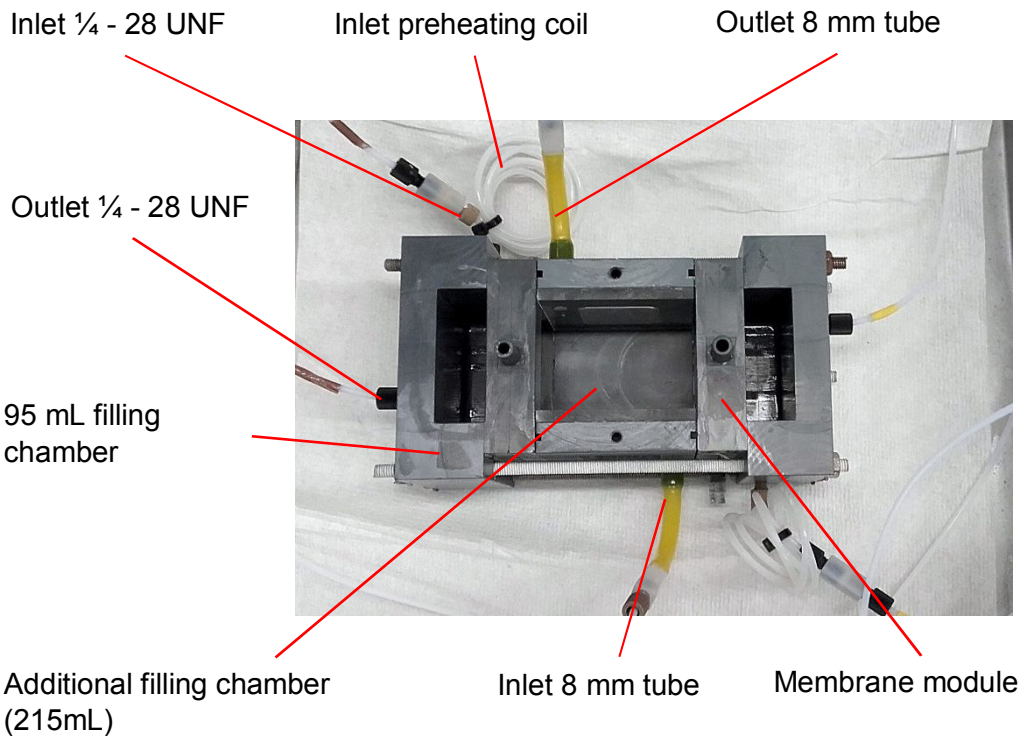


Fig. 3-4: Membrane reactor configuration with doubled exchange area. The outer chambers contain the organic phases, the middle chamber contains the aqueous phase.

The membrane reactor is started up by firstly impregnating the membrane module with either organic or aqueous phase. Therefore, the membrane module is positioned in a beaker and placed in an ultrasonic- bath for 30 minutes. If the membrane module and filling chamber are glued with epoxy resin, the whole compartment is placed in the ultrasonic- bath. After the ultrasonic treatment of the membrane module the surfaces are cleaned, the non- glued chamber is sealed with the densified PTFE flat sealing strip with a 3-5 mm distance to the inner edge. All parts are then assembled on the five threaded rods. To achieve an evenly distributed pressure along the seal face, the nuts are screwed hand tight at first and fastened with the same number of revolutions. Then the membrane reactor is connected to the peristaltic pumps. Optionally, pre- heating coils are installed prior to the inlet of the membrane reactor for elevated temperature experiments and whole setup is placed in the water bath.

First, the membrane reactor is filled with the phase that is not used to impregnate the membrane module. Membrane break- through is checked prior to filling in the second membrane phase. Subsequently the peristaltic pumps are turned on and the connections are checked for leaking. Finally, the sealing paste is spread around the opening in 3-5mm distance of the inner edge of the filling chambers and the lid is put on the reactor after the solvent of the sealing paste is evaporated.

### 3.2.2 Large Membrane Reactor

The main part of the large membrane reactor is the membrane module. Similar to the small membrane module, the large membrane module consists of two membrane frames made of PVC-U, where the membrane sheet is glued in between. In contrast to the small membrane reactor, the filling chambers are formed by the frame of the membrane module. Two openings on each side of the filling chambers are applied for inlet and outlet and hold ¼ - 28 UNF core threads. The membrane module is equipped with one inlet and outlet with ¼ - 28 UNF core threads. Similar to the small membrane reactor, the membrane sheet is a commercially available porous polyethylene sheet (pore size range of 7-12 µm and hydrophilic surface properties).

The filling chambers are closed with acryl glass lids which are sealed against the membrane module with *Viton*® caulking strips or densified PTFE flat sealing strips. Fig. 3-6 shows a detail view of the membrane reactor. The acryl glass lids and membrane module are joined by 22 bolts to achieve an equal contact pressure on the seal face. The different materials (acryl glass lids and PVC-U filling chamber) of the membrane reactor expand differently during heating. Since they are fastened tight together, the resulting stress would lead to cracks in the brittle acryl glass. Therefore, only experiments at room temperature are performed with this membrane reactor.

The membrane module is impregnated by placing it horizontally in a drip pan. Either organic or aqueous phase is firstly spread on the membrane using a Pasteur pipette. Once the whole membrane is equally wetted, more liquid is poured over the membrane so that the filling chamber is half filled. After the excess liquid has dripped through the membrane, the module is turned over and filled again with liquid. Subsequently, the membrane module is sealed with either caulking strip or densified PTFE flat sealing and closed with the acryl glass lids. Similar to the small membrane reactor, the screws need to be fastened equally. The membrane reactor is designed for continuous operation, but batch mode is possible by connecting inlet and outlet of each chamber with peristaltic pumps.

Sampling is achieved by a three-way valve at inlet and outlet of the membrane reactor. When a sample is taken, both peristaltic pumps are stopped and valves on the phase where the sample is taken, are opened. If one valve is closed, a pressure gradient along the liquid membrane could cause a membrane break- through. The sample is taken at the inlet valve of the

membrane reactor (outlet of the peristaltic pump) by temporary switching on the pump. To ensure that no air enters the membrane reactor, a container prior to the inlet of the pump is installed. Fig. 3-5 shows a flow chart of the large membrane reactor and indicates the sampling spot (top) and the setup with heterogeneous catalyst (bottom, pumps are not shown).

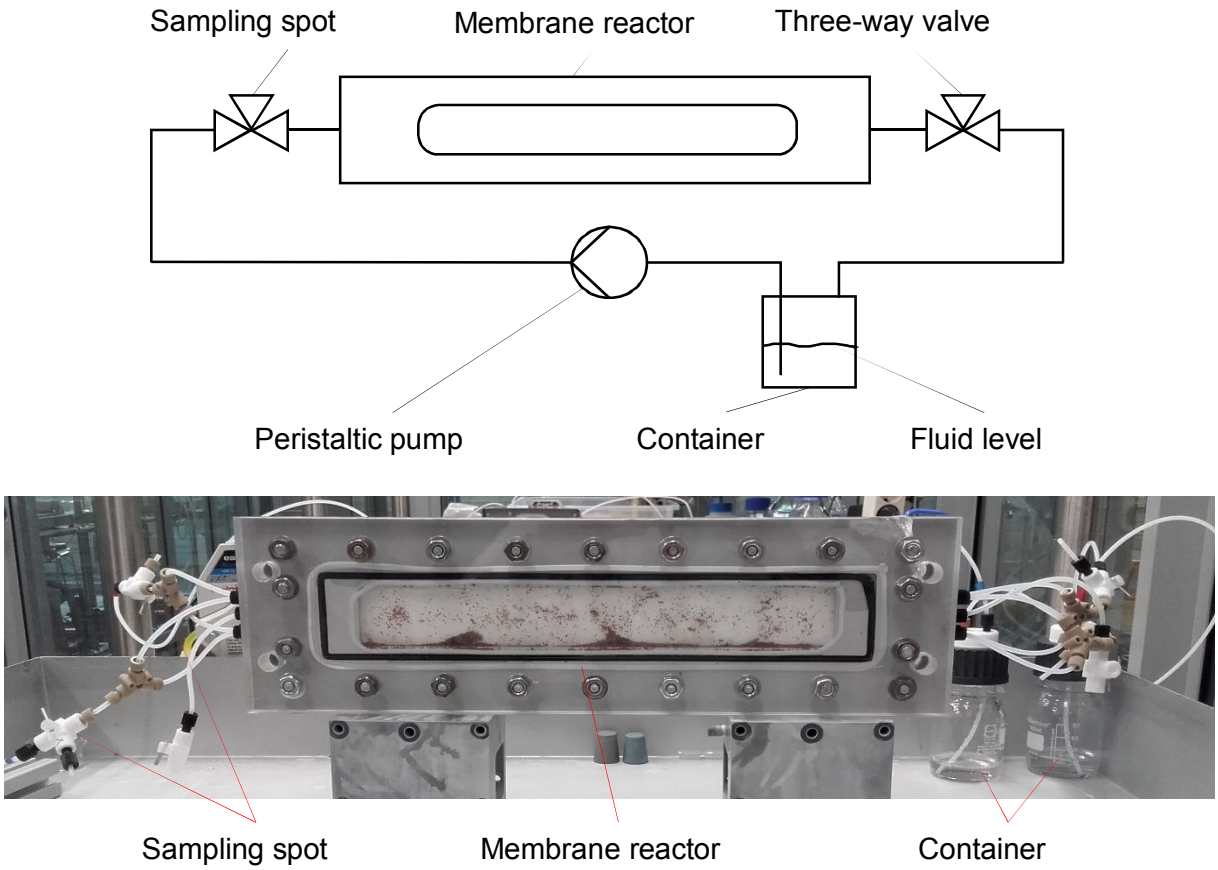


Fig. 3-5: Flow chart of large membrane reactor (top) and actual setup (bottom)

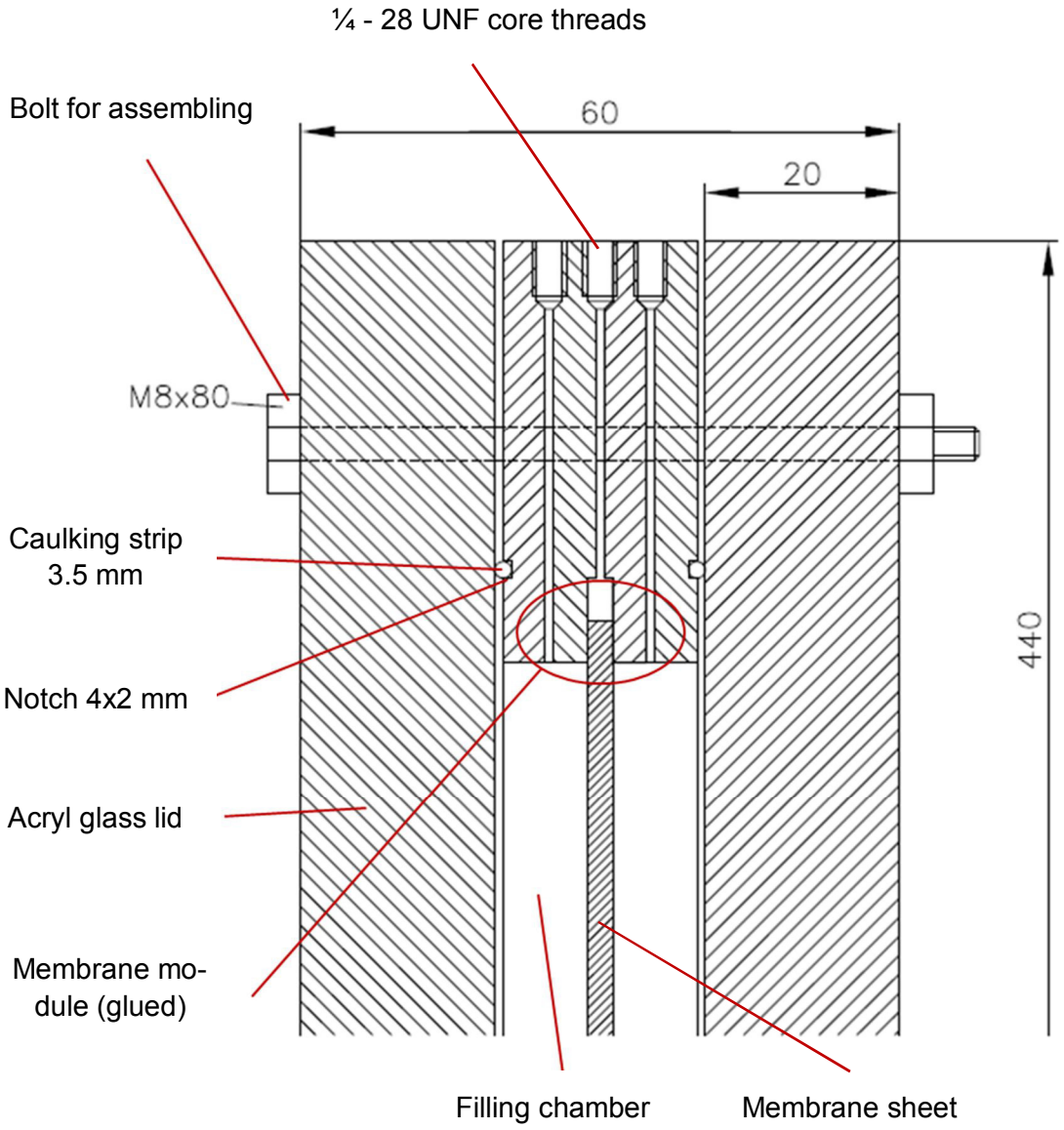


Fig. 3-6: Detail view of large membrane reactor. Adapted from [44]

## 3.3 Analytics

### 3.3.1 Measurement of Density and Dynamic Viscosity

The density and dynamic viscosity are measured with a *Stabinger Viscometer 3000* from *Anton Paar*, which combines the measurement of both parameters.

The density is measured with an oscillating U- tube which is electronically excited into undamped oscillation. When a sample is filled into the U-tube, it influences the eigenfrequency of the container depending on the sample mass. The density is calculated by comparison of the eigenfrequency of the filled U-tube and the two reference eigenfrequencies of air and deionized water. [45]

The measurement of dynamic viscosity is based on the Couette principle, where the sample is filled between two rotating cylinders. The outer tube rotates with a constant rotational speed and is filled with the sample fluid. Inside this tube, the measuring rotor with an integrated magnet floats freely in the fluid. Driven by the shear force of the sample (due to the rotation of the outer tube) the rotor experiences a torque, but magnetic effects retard this rotation. The rotor reaches stable rotational speed induced by the equilibrium of eddy current brake and the driving shear force. The equilibrium rotational speed is used to determine the viscosity of the sample [46]. Fig. 3-7 illustrates the measuring principle of the oscillating U- tube and Stabinger viscometer.

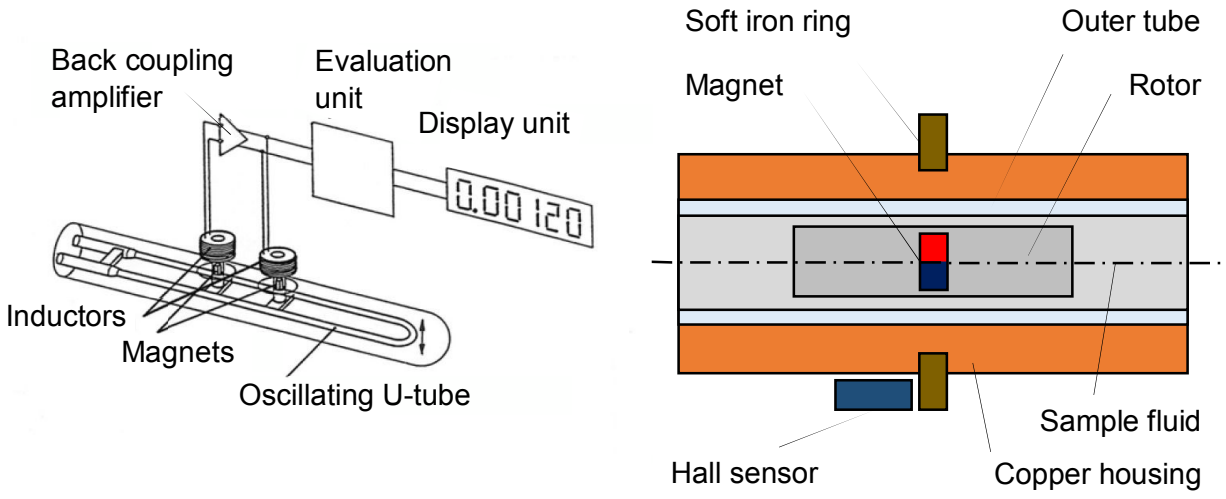


Fig. 3-7: Measuring principle of oscillating U- tube (left), adapted from [47] and Stabinger viscometer (right), adapted from [46]

### 3.3.2 Gas Chromatography and Calibration Factor

The samples are analyzed with an *Agilent 6890N* gas chromatograph (GC). The separation principle in gas chromatography is based on the different interactions of the analytes with the active layer inside the GC column.

The sample is evaporated in the injector and introduced into the GC column. The carrier gas (mobile phase), typically nitrogen or helium, transports the evaporated analytes through the column. The inner wall of the column is coated with an active microscopic layer of liquid, polymer or solid, known as stationary phase. Each analyte interact differently with the stationary phase and causes the compounds to eluate at specific times. The specific time that a compound needs to move through the column at defined conditions, is defined as retention time [48]. After the column, a flame ionization detector (FID) is installed. The flame is fueled by hydrogen and located at the outlet of the column. Carbon containing compounds are ionized by the flame to cations which are captured by the collector electrode (cathode). This causes a change in the current flow and leads to the signal in the chromatogram [49]. A general block flow diagram of a gas chromatograph and sketch of a FID is shown in Fig. 3-8.

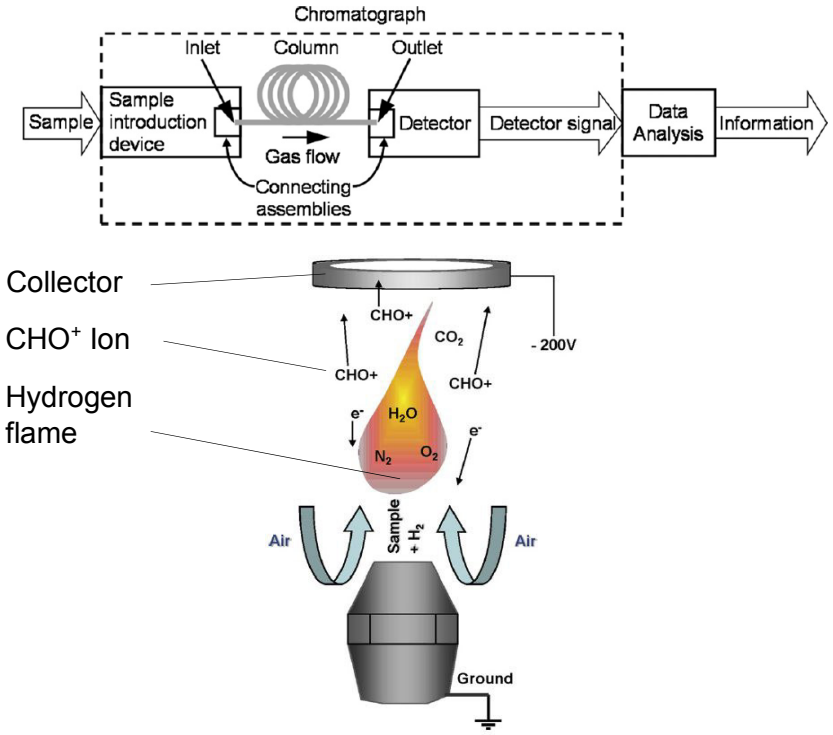


Fig. 3-8: Block diagram of gas chromatograph (top) [48] and sketch of flame ionization detector (bottom, adapted from [49])

The calibration factor $f_c$ is determined for each compound to be analyzed. Calibration of the GC is done with a dilution series with known mass fraction of the respective substance. The measured chromatograms are automatically integrated to obtain peak areas. A linear regression model ($y = k * x$) is used to correlate the mass fraction with the obtained peak areas. Mass fractions are plotted on the $y$- coordinate and peak areas are plotted on the $x$- axis. For each substance, the mass fraction is defined as:

$$w_i = \frac{m_i}{m_{total}} \quad \left[\frac{g_i}{g_{total}}\right] \tag{3-1}$$

The slope of the linear correlation represents the calibration factor $f_{c,i}$ for the specific substance $i$.

### 3.3.3 Sample Preparation and Sample Analysis

Taken samples are prepared prior to analysis. Aqueous samples are diluted in tetrahydrofuran (THF) with a ratio of 1:10 (w/w) while samples of the organic phase are diluted 1:20 (w/w) in *n*- heptane. The general procedure of sampling and sample preparation is described as follows. The mass of the empty GC vial is noted for each sample. Samples are taken with a pipette (100 µL for aqueous and 50 µL for organic samples), transferred to the vial and weighed. Then the sample is diluted with 1 mL of diluent and weighed again. The dilution factor $f_d$ is calculated according to equation 3-2.

$$f_d = \frac{m_{diluted\ sample} - m_{empty\ vial}}{m_{sample+vial} - m_{empty\ vial}} = \frac{m_{total}}{m_{sample}} \quad \left[\frac{g_{total}}{g_{sample}}\right] \tag{3-2}$$

To determine the mass fraction of a compound $i$ in the sample, the obtained peak area of the respective substance is multiplied with the calibration and dilution factor. The units are indicated in equation 3-3, using equations 3-1 and 3-2.

$$[w_i] = Area_i * f_{c,i} * f_d = pA * min * \frac{w_i}{pA*min} * \frac{g_{total}}{g_{sample}} = \left[\frac{g_i}{g_{sample}}\right] \tag{3-3}$$

# 4 Experiments

The aim of this work was to assess the applicability of supported liquid membranes for the removal of carboxylic and hydroxycarboxylic acids from diluted aqueous systems. Acetic acid solution with a concentration of 60 g/L was used as a standard model system. The organic phase was composed of *n*- octanol, aliphatic hydrocarbon solvent, either *n*- undecane or *n*- heptane and as catalysts DBSA, Amberlyst, deep eutectic solvent and sulfuric acid were used. The solubility *n*- octanol in the aqueous phase is negligible and hence used for the experiments. Preliminary experiments with the catalyst DBSA lead to emulsion formation in conventional liquid/ liquid extraction processes.

To define a starting point and conditions for the membrane reactor experiments, preliminary experiments were performed. In the first step, one phase experiments in the organic phase were performed to assess the applicability of different catalysts for the esterification of acetic acid with *n*- octanol. Next, the reaction was transferred to two-phase contact in a three-neck flask, with acetic acid in the aqueous and *n*- octanol and the catalyst in the organic phase. In conventional liquid/ liquid extraction, the mass transfer area and hence the mass transfer rate are high compared to the available membrane reactor. Hence, these experiments were performed to determine, if a membrane reactor would be necessary for the defined separation task. To increase the concentration of acetic acid in the organic phase, the reactive extraction agent trioctylamine (TOA) was used. TOA is used for the reactive extraction of organic acids. The influence of TOA on the extraction and esterification in the organic phase using Amberlyst

Based on the preliminary experiments, the reaction system was transferred to the liquid membrane reactor setup. The modular design of the reactor allows to perform experiments at different A/V phase ratios. The majority of the membrane reactor experiments was performed with organic SLM and organic receiving phase. To evaluate the effect of the membrane phase on the removal of acetic acid from the feed phase, additional experiments were performed using aqueous- phase SLM and organic receiving phase. Experiments were conducted to find the critical concentration of DBSA, with regards to emulsion formation in the aqueous feed phase. Physical extraction of acetic acid into the organic phase in the membrane reactor was investigated using *n*- octanol as modifier and reactant and Amberlyst® 15 as catalyst.

## 4.1 Preliminary Experiments

### 4.1.1 One-Phase Esterification of Acetic Acid with *n*-Octanol and Variation of Catalyst

Experiments were performed in the apparatus described in section 3.1. The organic phase consisted of aliphatic solvent, either *n*- undecane or *n*- heptane and *n*- octanol at double molar excess with respect to acetic acid. Previous experiments showed that the solvent did not affect the reaction [50]. The catalyst was chosen in consideration of subsequent application in the membrane reactor. For homogeneous catalysis, DBSA was selected whereas Amberlyst® 15 was used for heterogeneous catalysis. Novel Deep Eutectic Solvent (DES) used as dual solvent-catalyst was investigated for possible application. The amount of catalyst was 10 w% based on the total mass of the organic phase for DBSA and 3 w% and 10 w% for Amberlyst® 15. The concentration of DBSA was not varied in the one phase experiment due to emulsion formation in direct two phase contact. Emulsion formation was further studied in membrane reactor experiments (see section 4.2.1). The procedure for DES deviated from the experiments with Amberlyst® 15 and DBSA and are described separately in this section. The concentration of acetic acid was 60 g/L. This was reasoned by similar concentrations found in the effluents of the pulp and paper industry [4]. Tab. 4-1 summarizes the performed experiments.

Tab. 4-1: Overview of one-phase experiments

| | A1 | A2 | A3 | A4 |
|---|---|---|---|---|
| Catalyst | DBSA | Amberlyst® 15 | Amberlyst® 15 | DES |
| Amount | 10 w% | 10 w% | 3 w% | N/A |
| Solvent | *n*-undecane | *n*-undecane | *n*-heptane | DES |
| Acetic acid concentration | | 60 g/L | | 90 g/L |
| Molar ratio acid: alcohol | | 1:2 | | 1:1 |
| Alcohol | | *n*-octanol | | *n*-octanol |
| Temperature | | 50°C | | 60°C |

The solvent, *n*-octanol and the catalyst were filled in the 500 mL flask and heated up to 50°C. After reaching the temperature, acetic acid was added and temperature dropped by 2 to 3°C. Immediately after all substances were added, the first sample was taken using a disposable needle. If Amberlyst® 15 was used, the sample was filtered through a syringe filter (PTFE 0.45 µm) prior to transfer to the vial. Samples were taken at 0, 30, 60, 90, 120 and 180 minutes after reaction was started and subsequently prepared as described in section 3.3.3. Samples containing DBSA were cooled on ice prior to analysis.

The deep eutectic solvent which functioned as solvent and catalyst was prepared by mixing equimolar amounts of *p*-Toluenesulfonic acid monohydrate (PTSA) and trimethylcyclohexyl ammonium methanesolfonate (TCyAMsO) with mortar and pestle. Next, the resulting white paste was transferred to a 10 mL vial, heated up to 60°C while magnetically stirred, until a clear liquid was obtained (after 10 minutes). An addition of both salts into a vial while stirring and heating as described by De Santi et al [32], resulted in a suspension with white crystals and clear liquid even after three hours at 60°C.

The quaternary ammonium methanesulfonate salt TCyAMsO was prepared following the description in [32]. Equimolar amounts (0,12 mol) of *N,N*-Dimethylcyclohexylamine and methyl methansulfonate were dissolved in 150 mL ethyl acetate. As soon as the second compound was added to the solution, the first, needle shaped, crystals precipitated. The mixture was slightly stirred several times and heat generation was observed. After 60 minutes of reaction time, the precipitated solid was filtrated, washed twice with diethyl ether and dried in vacuum for 24 hours to result in a white crystalline solid. A yield of 85 % was achieved. This solid was used without further treatment in the preparation of the DES.

The experiment with DES was conducted related to the description in [32]. First, 3 mL of DES were filled in a 10 mL vial and 4.5 mmol *n*-octanol was added and heated up to 60°C under constant stirring. Then 4.5 mmol acetic acid was added. Assuming that both alcohol and acid were soluble in DES, the initial acid concentration was 90 g/L. Samples were taken after 60 minutes and prepared as described in section 3.3.3.

Solubility of DES was investigated by adding 50 µL DES to either 10 mL deionized water or *n*- undecane and mixing it three minutes using a vortex mixer.

### 4.1.2 Two-Phase Esterification of Acetic Acid with *n*-Octanol and Variation of Catalyst

Experiments with direct two-phase contact were performed using the same apparatus as for the one-phase experiments. The aqueous phase consisted of 60 g/L acetic acid in deionized water, the organic phase was *n*-octanol in *n*-undecane or *n*-heptane with a phase ratio of 1:1 (v/v) for all experiments. The concentration of *n*-octanol was based on double molar excess with respect to acetic acid. Three different catalysts were used, Amberlyst® 15, sulfuric acid and DBSA. Catalyst concentration was 10 w% with respect to the organic phase for Amberlyst® 15 and 0.01 mol/L for sulfuric acid in the aqueous phase. The concentration of DBSA was varied. Tab. 4-2 summarizes the performed experiments.

To start the experiments, water, catalyst and organic phase were filled in the three-neck flask and heated up to 50°C. The reaction was started by adding acetic acid to the system. Samples were taken at predefined time intervals after addition of acetic acid. The stirrer was stopped and after the phases were separated, samples were taken using a needle on a 1 mL syringe. Sample volume was 300 µL for each phase to keep the phase ratio constant. The samples were filtrated through a syringe filter and prepared as described in section 3.3.3.

Tab. 4-2: Overview of two-phase experiments

| | B1 | B2 | B3 | B4 | B5 |
|---|---|---|---|---|---|
| Catalyst | DBSA | DBSA | DBSA | Amberlyst® 15 | Sulfuric acid |
| Amount | 0.1 w% | 1 w% | 5 w% | 10 w% | 0.01 mol/L |
| Solvent | n-undecane | | | n-heptane | n-undecane |
| Acetic acid concentration | 60 g/L | | | | |
| Molar ratio acid: alcohol | 1:2 | | | | |
| Alcohol | n-octanol | | | | |
| Phase ratio | 1:1 (v/v) | | | | |
| Temperature | 50°C | | | | |

### 4.1.3 Reactive Extraction combined with Esterification in Two-Phase System

The influence of trioctylamine on the esterification of acetic acid and reactive extraction of acetic acid into the organic phase was investigated using the setup described in section 3.1. One-phase experiments were performed using*n*-octanol at double molar excess with respect to acetic acid and *n*-heptane as solvent and acetic acid at 60 g/L. The concentration of TOA and Amberlyst® 15 was varied to investigate the interaction of TOA with Amberlyst® 15. In the two-phase experiment, the aqueous phase was acetic acid in water with a concentration of 60 g/L and the organic phase consisted of *n*-octanol at double molar excess using *n*-heptane as solvent. Catalyst concentration was 10 w% based on the organic phase and TOA was added in a molar ratio of 0.1:1 with respect to acetic acid. Tab. 4-3 summarizes the performed experiments.

The one-phase experiments were started by adding acetic acid to the preheated mixture. Samples were taken 30, 60, 90, 120 and 180 minutes after the reaction was started. Two-phase experiments were started by the addition of acetic acid and TOA and samples were taken at the same intervals as for one-phase experiments. Due to the use of Amberlyst® 15, all samples were filtrated through a syringe filter prior to preparation as described in section 3.3.3.

Tab. 4-3: Overview of reactive extraction experiments

| | C1 | C2 | C3 | C4 | C5 | C6 |
|---|---|---|---|---|---|---|
| Molar ratio TOA: acid | 0 | 0 | 1:10 | 1:10 | 1:1 | 1:10 |
| Molar ratio TOA: catalyst | 0 | 0 | 1:1 | 1:3 | 3:1 | 1:3 |
| Amount Catalyst[1] | 10 w% | 3 w% | 3 w% | 10 w% | 10 w% | 10 w% |
| Phase ratio | one phase | | | | | 1:1 (v/v) |
| Solvent | *n*-heptane | | | | | |
| Acetic acid concentration | 60 g/L | | | | | |
| Molar ratio acid: alcohol | 1:2 | | | | | |
| Alcohol | *n*-octanol | | | | | |
| Temperature | 50 °C | | | | | |

[1] Amberlyst® 15, amount with respect to organic phase.

### 4.1.4 Physical Extraction of Acetic Acid with Variation of *n*-Octanol Mass Fraction

The effect of *n*-octanol on the extraction of acetic acid from the aqueous phase was studied. Therefore, experiments in heated separation funnels (50°C) were performed in which the distribution of acetic acid between the aqueous and organic phase at a phase ratio of 1:1 (v/v) was analyzed. Based on [51], it was assumed, that the equilibrium was reached after 60 minutes. The aqueous phase consisted of 60 g/L acetic acid in deionized water and the concentration of *n*-octanol in the organic phase was varied with *n*-undecane as solvent. Tab. 4-4 summarizes the performed experiments.

The experiments were started by filling 30 mL of each phase into the preheated separation funnels and set the shaking interval to 150 swings per minute. After 60 minutes, the device was stopped and phases were allowed to separate for 15 minutes. The phases of experiments containing 80 w% and pure *n*-octanol were separated for 5 minutes using a table centrifuge at 250 rpm. Samples of both phases were taken and prepared as described in section 3.3.3. Density and dynamic viscosity were measured according to section 3.3.1.

Tab. 4-4: Overview of physical extraction experiments

| | D1 | D2 | D3 | D4 | D5 | D6 |
|---|---|---|---|---|---|---|
| *n*-octanol in org. phase | 0 w% | 20 w% | 33,8 w% | 60 w% | 80 w% | 100 w% |
| Organic phase solvent | *n*-undecane | | | | | |
| Aqueous phase | 60 g/L acetic acid | | | | | |
| Phase ratio | 1:1 (v/v) | | | | | |
| Temperature | 50 °C | | | | | |

## 4.2 Experiments in the Two- Phase Membrane Reactor

This part of the work focuses on membrane reactor experiments wherein the membrane phase was the same as either the feed or the receiving phase. This configuration is further described as two-phase membrane reactor. Feed and receiving phase are immiscible. In the original concept of supported liquid membranes, the membrane phase separates two miscible phases and many applications exist where an organic phase SLM separates two aqueous phases [43]. The membrane stability is the crucial attribute of the membrane reactor and the challenge of a stable SLM is eliminated, if the membrane phase is identical with either feed or receiving phase.

In the two- phase membrane reactor, both, heterogeneous and homogeneous catalysts in the organic phase were used. DBSA was chosen for homogeneous and Amberlyst® 15 for heterogeneous catalysis.

Fig. 4-1 gives an overview of the reaction systems performed with the membrane reactor. The performed experiments are subsequently described and classified according to the used catalyst, which was DBSA for homogeneous and Amberlyst® 15 for heterogeneous catalysis.

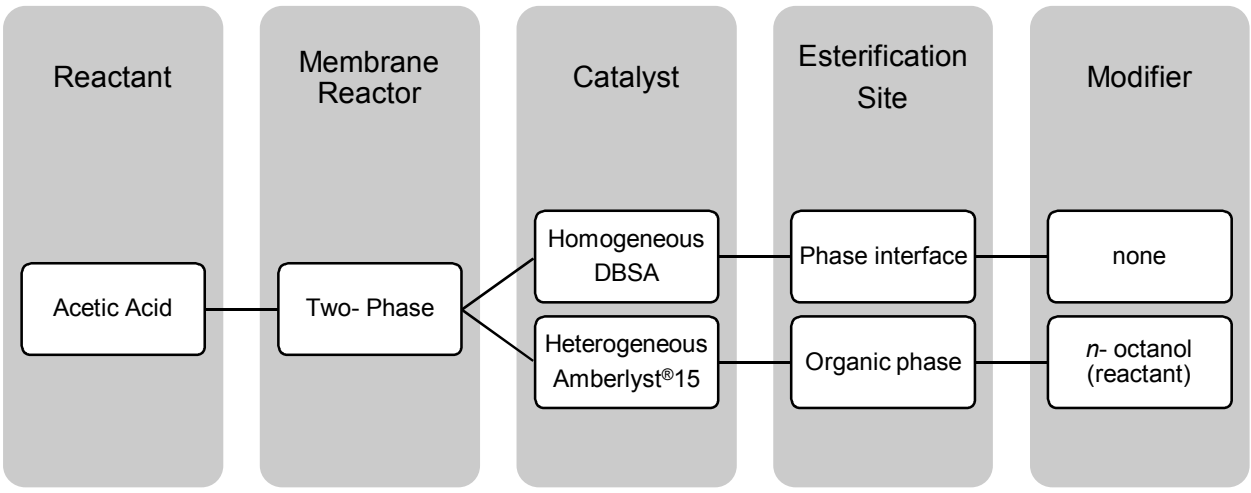


Fig. 4-1: Overview of membrane reactor experiments

### 4.2.1 Homogeneous Catalysis in the Two- Phase Membrane Reactor

The developed model concept in section 2.5 was the basis for the experiments which used DBSA in the membrane reactor. The reason for using the membrane reactor instead of direct two-phase contact in a stirred vessel was the tendency of DBSA to form stable emulsions. With establishing a rigid phase interphase by means of a supported liquid membrane, it was possible to reduce emulsion formation, depending on the concentration of DBSA. Since DBSA is almost insoluble in water [52], one important characteristic of the system was the concentration of DBSA in the organic phase, at which no emulsion was observed in the contacted aqueous phase.

One set of experiments determined the critical concentration of DBSA in the membrane reactor. Above the critical DBSA concentration, emulsion formation was observed. The emulsion formation is defined by the first recognizable turbidity of the aqueous phase within 24 hours of reaction time at 20°C. The critical DBSA concentration determined in these experiments is not related to the critical micelle concentration (CMC) mentioned in section 2.2. The CMC is defined in a mixed two-phase system and represents the concentration in which the properties of the emulsion change abruptly [34]. In contrast, the critical DBSA concentration represents the concentration of DBSA initially present in the organic phase at which no emulsion formation in the aqueous phase is observed and its applicability is limited to the membrane reactor setup.

The aqueous phase contained 60 g/L acetic acid. The organic phase consisted of *n*-octanol at double molar excess with respect to acetic acid at a phase ratio (organic: aqueous) of 1:2 (v/v) for the small and 1:1 (v/v) for the large membrane reactor and *n*-undecane as solvent. The catalyst DBSA was added to the organic phase in variable concentrations, which are summarized in Tab. 4-5. Experiments were performed with organic and aqueous membrane phase. At first, the critical DBSA concentration was determined for stagnant phases using the small membrane reactor described in section 3.2.1. Next, both phases were circulated using peristaltic pumps.

The energy input (imposed convection) into the system is characterized by the inlet velocity $v$ of the fluid which is related to the mean residence time according to equation 4-1. The mean residence time $\tau$ is independent of the used membrane configuration and thus the chosen parameter to relate emulsion formation with energy input.

$$\tau = \frac{V}{\dot{V}} = \frac{V}{v * A_{in}} \quad [min] \tag{4-1}$$

The pump was operated at the same flow rate for all experiments, hence the mean residence time $\tau$ for the aqueous phase of the small membrane reactor was $\tau =$ 7.5 min and $\tau =$ 3.8 min for the large membrane reactor.

Experiments in the large membrane reactor (see section 3.2.2) were performed, but instead of vertically opposite phases, the SLM separated both phases horizontally, with the organic phase on top. Only the aqueous phase was circulated in that configuration.

Tab. 4-5: Overview of used DBSA concentrations (in w%) in membrane reactor experiments

| Membrane reactor | small | | large | |
|---|---|---|---|---|
| Membrane phase | organic | aqueous | organic | aqueous |
| Stagnant | 2.5; 3.0; 3.25; 3.5; 4.0; 5.0 | - | 3 | - |
| Circulated | 1; 3 | 1; 2; 3 | - | 1; 2 |

The membrane reactors were set up as described in section 3.2 and observed in time intervals of 60 minutes. In the small membrane reactor, the 215 mL filling chamber equipped with the sight window was used for the aqueous phase to observe the emulsion formation. The organic phase was filled in the 95 mL chamber.  illustrates the reactor configurations which were used to determine the critical DBSA concentration. Samples were taken when emulsion formation was observed or after 24 hours of reaction time and were prepared as described in section 3.3.3.

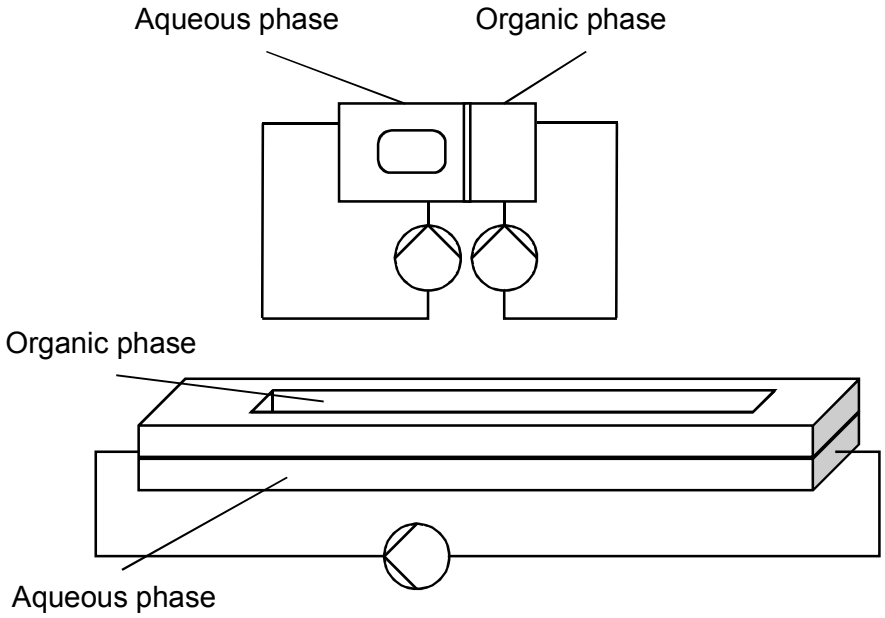


Fig. 4-2: Membrane reactor configurations. Top: Small reactor with 215 ml aqueous phase and 95 ml organic phase and both phases circulated. Bottom: large reactor and only aqueous phase circulated

### 4.2.2 Heterogeneous Catalysis in the Two- Phase Membrane Reactor

The other set of experiments in the membrane reactor investigated its applicability for the extraction of acetic acids through the supported liquid membrane and esterification in the receiving phase. Amberlyst® 15 was used as heterogeneous catalyst. Similar to the experiments in section 4.2.1, the membrane phase was the same as either feed or receiving phase for one set of experiments.

For the two-phase experiments, both small and large membrane reactors were used. Experiments in the small membrane reactor were performed at 20°C and 50°C, whereas experiments in the large membrane reactor were only conducted at 20°C (see section 3.2.2). In all two-phase experiments, the organic phase consisted of *n*-octanol (33.8 w%) and *n*-undecane as solvent. The concentration of *n*-octanol is equal to the double molar excess of 60 g/L acetic acid solution at a phase ratio of 1:1 (v/v). The concentration of acetic acid in the aqueous phase was varied from 60 g/L to 480 g/L. Amberlyst® 15 was added to 2 w% with respect to the organic phase. Tab. 4-6 summarizes the performed two-phase experiments.

Tab. 4-6: Overview of two-phase membrane reactor experiments

| Membrane reactor | small | | large |
|---|---|---|---|
| Area/ Volume ratio | 0.26 $cm^{-1}$ | | 1.11 $cm^{-1}$ |
| Temperature | 20°C | 50°C | 20°C |
| Acetic acid concentration | 60 g/L | 60 – 480 g/L | 60 g/L |
| Molar ratio acid: alcohol | 1:2 | variable | 1:2 |
| Alcohol | *n*-octanol | | |
| Solvent | *n*-undecane | | |
| Phase ratio | 1:1 (v/v) | | |
| Amberlyst® 15 | 2 w% | | |

In the two-phase membrane reactor experiments, the reactors were set up as described in section 3.2. The small membrane module was either impregnated by placing a beaker containing the membrane module and membrane phase in the ultrasonic bath or impregnated similar to the large membrane module. No difference in reactor performance was observed with the different impregnation methods. After connecting the peristaltic pumps to the small modules and filling in both phases, the catalyst was added to the organic phase by pouring it into the filling chamber. The flow rate of the pump for the organic phase was adjusted such, that the catalyst particles were slightly moved but not swirled up to the outlet of the filling chamber at the top of the reactor. Samples were taken from both phases at defined time intervals and prepared according to section 3.3.3. The large membrane reactor was set up as described in section 3.2.2. After impregnating the membrane, a fiberglass wool was spread out in the organic phase filling chamber before the catalyst was added. This ensured a more even distribution of the catalyst which is shown in Fig. 4-3.

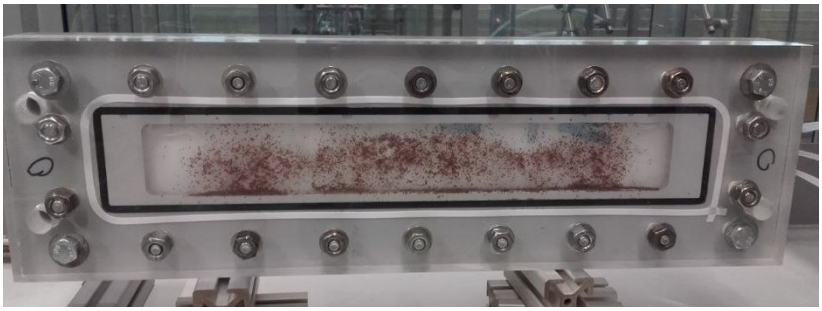

Fig. 4-3: Distribution of catalyst in the large membrane reactor

# 5 Results and Discussion

The conversion of acetic acid $X_{HAc,t}$ at reaction time $t$ was calculated according to equation 5-1:

$$X_{HAc,t} = \frac{n_{HAc,0} - n_{HAc,t}}{n_{HAc,0}} * 100\% = \frac{n_{OcAc,t}}{n_{HAc,0}} * 100\% \quad (5\text{-}1)$$

$n_{HAc,0}$ is the initial amount of acetic acid, $n_{HAc,t}$ the amount of acetic acid and $n_{OcAc,t}$ the amount of formed octyl acetate at time $t$.

## 5.1 Preliminary Experiments

### 5.1.1 One-Phase Esterification of Acetic Acid with *n*-Octanol and Variation of Catalyst

One-phase experiments were performed to assess the applicability of different catalysts for subsequent use in the membrane reactor. Fig. 5-1 compares the conversion of acetic acid using different catalysts and different catalyst amounts. For experiments A1- A3, the acetic acid concentration was 60 g/L and for A4 90 g/L (see section 4.1.1). The homogenous catalyst DBSA and dual solvent-catalyst DES showed almost complete conversion after 60 minutes of reaction time. The heterogeneous catalyst Amberlyst® 15 achieved less than 50 % conversion at the same time, but conversion increased with increasing reaction time. After 180 minutes, 82.2 % conversion was obtained using 10 w% Amberlyst® 15.

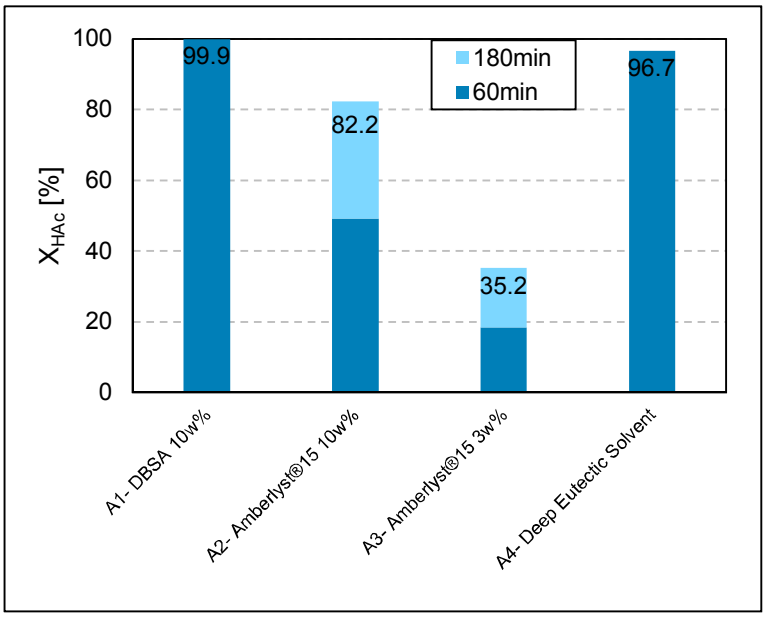


Fig. 5-1: Conversion of acetic acid with various catalysts in one-phase esterification at 50°C and ambient pressure

Tab. 5-1 compares the ratio of acid to catalyst for the experiments A1- A4. The higher the ratio, the more acetic acid needs to be converted per mol of catalyst. In the case of Amberlyst® 15, a concentration of active sites of 4.7 mol/kg was assumed, as this represents the maximum concentration according to [53]. In both Amberlyst® 15 and DBSA, the active site was sulfonic acid. It can be seen in Tab. 5-1, that the molar ratio for DBSA (A1) is in between the ratio of Amberlyst® 15 (A2 and A3) but Fig. 5-1 shows higher conversion of acetic acid with DBSA than Amberlyst® 15. Homogeneous catalysts show, in general, higher reaction rates than comparable heterogeneous catalysts since the catalyst is homogeneously distributed in the solution and diffusion of the reactants into the catalyst pores is not necessary[24], [54]. The increase of conversion using Amberlyst® 15 at prolonged reaction time indicated a diffusion limitation rather than deactivation. Since both catalysts bare the same active site, it can be assumed that catalyst deactivation due to the byproduct water was of similar extent [29], [55]. Based on these findings, it can be concluded that DBSA is a more efficient catalyst for the esterification of acetic acid with *n*-octanol than Amberlyst® 15.

The direct comparison of DES with DBSA and Amberlyst® 15 was not suitable since DES was used as dual solvent- catalyst, however the experimental results are shown in Tab. 5-1 and Fig. 5-1. The reason for investigating DES was to assess its applicability in the membrane reactor, for example as membrane phase or solvent and liquid catalyst.

Tab. 5-1: Ratio of acid/ catalyst for one-phase esterification

| | A1 | A2 | A3 | A4 |
|---|---|---|---|---|
| Catalyst | DBSA | Amberlyst® 15 | | DES |
| Initial mass acetic acid [g] | 9.33 | 9.39 | 9.11 | 0.27 |
| Catalyst loading [w%] | 10 | 10 | 3 | N/A |
| Amount catalyst [mol] | 0.037 | 0.055 | 0.014 | 0.009 |
| Ratio acid: catalyst [mol/mol] | 4.15 | 2.82 | 10.80 | 0.49 |

The experiments were performed in organic phase for A1-A3, thus the byproduct water of the esterification (see section 2.1) was constantly removed from the reaction system, enabling a conversion higher than equilibrium conversion. Although DBSA facilitates emulsion formation in a two-phase system, no emulsion formation was observed for experiment A1. This might be

reasoned by the relatively large amount of DBSA compared to the produced water. At 99.9 % conversion, only 2.8 g of water are formed which do not affect the system of 150 mL reaction mixture and 12.2 g of DBSA.

In experiment A4, a heterogeneous system was formed with proceeding reaction time. The added *n*-octanol was completely miscible and seemed to be dissolved in the DES. The mixture turned turbid 4 minutes after adding acetic acid and a phase separation was noticed after 20 minutes, with both phases turbid. The upper phase was clear after 60 minutes, whereas the lower phase remained turbid. This observations coincide with the findings in [32], in which the authors point out, that the produced ester is not soluble in the DES phase. The performed dissolution test in which 50 µL DES where dissolved in either deionized water or *n*-undecane showed that DES was soluble in water, but remained as a separate phase in the aliphatic solvent. The turbidity might be explained by the presence of water and *n*- octanol in the DES phase. Due to its hydroxyl group, *n*- octanol can act as a surfactant similar to other anionic surfactants which leads to emulsion formation under energy input by means of mixing (see section 2.2).

### 5.1.2 Two-Phase Esterification of Acetic Acid with *n*-Octanol and Variation of Catalyst

Direct two- phase contact in batch experiments using different catalysts was studied to evaluate if a subsequent translation of the reaction matrix to the membrane reactor is even necessary. Tab. 5-2 summarizes the obtained results. In direct two- phase contact and stirring, DBSA induced emulsion formation even at low catalyst concentration of 0.1 w% with respect to the organic phase. The emulsions did not separate after 10 minutes of centrifuging (250 rpm) and were stable for at least seven days (after seven days, the emulsions were disposed). Due to emulsification of the system, no analysis of experiments B1-B3 was possible. No emulsion was formed in experiment B4, using Amberlyst® 15 and the emulsion produced in B5 using sulfuric acid in the aqueous phase, separated completely within 20 seconds after the stirrer was stopped.

Tab. 5-2: Conversion of acetic acid and distribution of alcohol and acid between aqueous and organic phase at 50°C and ambient pressure

| | B1 | B2 | B3 | B4 | B5 |
|---|---|---|---|---|---|
| Catalyst | DBSA | DBSA | DBSA | Amberlyst® 15 | Sulfuric acid |
| Amount | 0.1 w% | 1 w% | 5 w% | 10 w% | 0.01 mol/L |
| Molar ratio acid: catalyst | 423.7 | 42.4 | 8.4 | 3.2 | 101.2 |
| *n*- octanol in aq. phase[1] | N/A | N/A | N/A | 0.1±0.02 w% | 0.1±0.01 w% |
| Acetic acid in org. phase[1] | N/A | N/A | N/A | 13.3±1.3 w% | 7.2±1.7 w% |
| Conversion after 180min | N/A | N/A | N/A | 0.19 % | 0.78 % |

[1] averaged over reaction time

Physical extraction of acetic acid into the organic phase was observed in experiments B4 and B5. Fig. 5-2 shows the conversion of acetic acid over time and its distribution between aqueous and organic phase for experiments B4 (Amberlyst® 15) and B5 (sulfuric acid). The distribution was calculated by dividing the total mass of acetic acid in the respective phase by the initial mass of introduced acid. It can be seen, that the relative distribution remains approximately constant despite the reaction of acetic acid in the system (Fig. 5-2, right). The averaged distribution of acetic acid and *n*- octanol over reaction time are summarized in Tab. 5-2. The long chain *n*- octanol was almost completely present in the organic phase and only 0.1 % of the introduced alcohol was found in the aqueous phase for both B4 and B5. In contrast, approximately 85 % (relative) more acetic acid was present in the organic phase using Amberlyst® 15 as catalyst instead of sulfuric acid. This might be explained by the strong acidity of sulfuric acid [56] which induce protonation of the weaker acidic acid in the aqueous phase [25]. The protonation prevents acetic acid to migrate into the organic phase [37], which explains the different concentrations of acetic acid in the organic phase in B4 and B5.

The conversion of acetic acid for both B4 and B5 was below 1 % after 180 minutes reaction time (Tab. 5-2 and Fig. 5-2). The formation of octyl acetate during the experiments was monitored with gas chromatography and was below the instruments limit of quantitation for B4 (30-120 minutes), but above the detection limit. No octyl acetate was found in the aqueous phase in both B4 and B5 (below detection limit). Since both reactants and sulfuric acid were present in the aqueous phase in experiment B5, the esterification most likely occurred in that phase.

The resulting ester was immiscible with water and dissolved in the organic phase. The low conversion might be explained by the low concentration of alcohol (0.03 w%) in the aqueous phase. In experiment B4, the concentration of *n*- octanol in the aqueous phase was similar to B5 but the formation of a hydration sphere around the active site of the catalyst [55] might have hindered adsorption of the reactants, thus decreasing esterification rate. The formation of a hydration sphere around the sulfonic acid group was likely since the catalyst was fully immersed in the aqueous phase each time the stirrer was stopped for sampling. If the contact of aqueous phase and catalyst is avoided or reduced, higher conversions are possible as stated in [51].

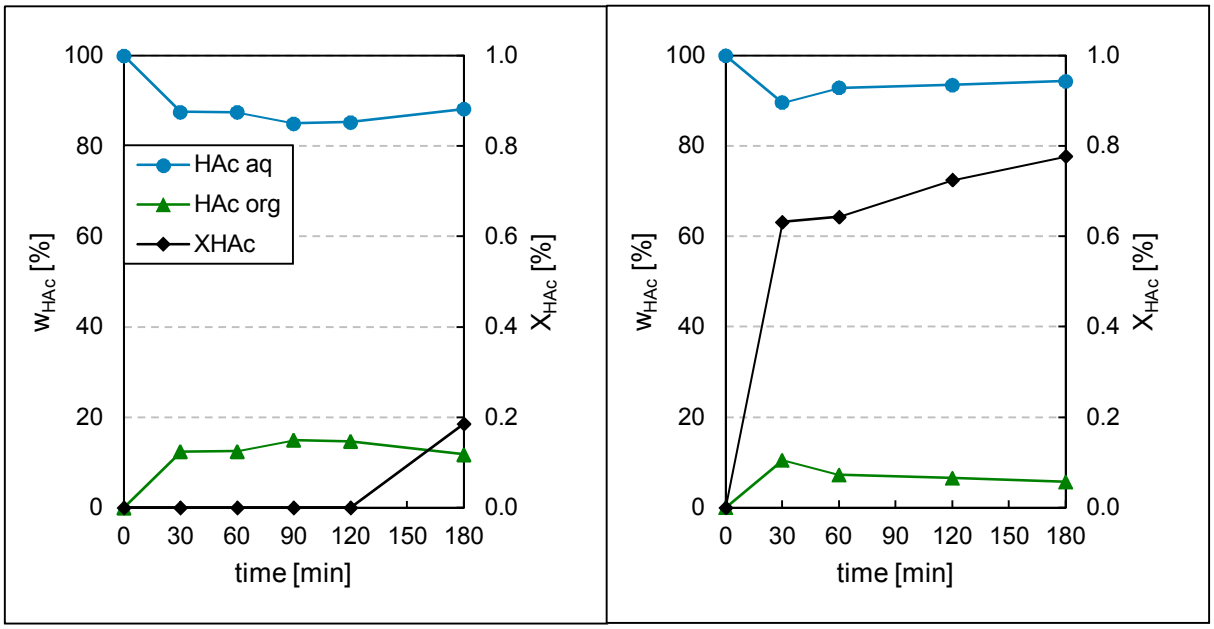


Fig. 5-2: Distribution of acetic acid in aqueous (blue) and organic (green) phase and conversion (black) of acetic acid using Amberlyst® 15 (left) and sulfuric acid (right) at 50°C and ambient pressure

Direct two- phase contact under constant stirring was not feasible using DBSA as catalyst due to emulsion formation. Although conversion of acetic acid was achieved using Amberlyst® 15 or sulfuric acid, direct two- phase contact did not show to be efficient. In addition, a subsequent phase separation has to be taken into account as well as a contamination of the aqueous stream with catalyst is the consequence if sulfuric acid is used.

### 5.1.3 Reactive Extraction combined with Esterification in Two-Phase System

Since direct two- phase contact described in section 5.1.2 did not yield to considerable reduction of acetic acid in the aqueous phase, the utilization of the reactive extracting agent TOA in the system was studied.

Fig. 5-3 illustrates the conversion of acetic acid and distribution between aqueous and organic phase for experiment C6 (see Tab. 4-3). Similar to the comparable experiment B4 (Fig. 5-2, left), the conversion was around 0.2 % and octyl acetate was below the limit of quantitation until 120 minutes of reaction time. The distribution of acetic acid between both phases was similar to experiment B4. The concentration of 5 w% TOA in the organic phase was expected to lead to a higher amount of extracted acid, as studies show in which a mixture of amines was used [40], [57] to extract low concentrated acetic acid from an aqueous phase.

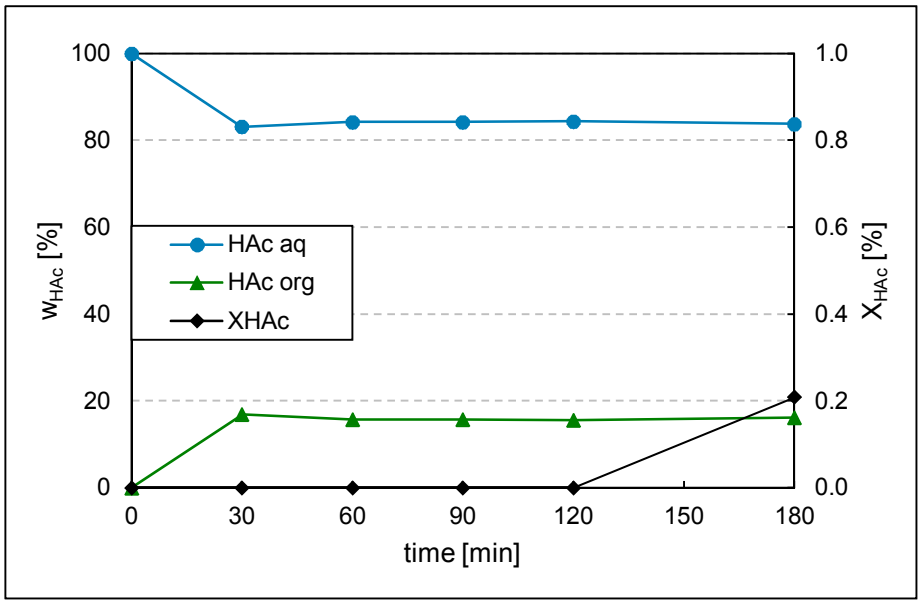


Fig. 5-3: Conversion of acetic acid (black) in two-phase system (C5) using 10 w% Amberlyst® 15 and distribution of acetic acid between aqueous (blue) and organic phase (green) at 50°C and ambient pressure

At the beginning of the experiment, when both phases were added to the flask (except TOA and acetic acid), Amberlyst® 15 was well dispersed in both phases due to mixing. Right after the addition of TOA, the catalyst flocculated immediately to larger conglomerates. When stirring was stopped, the catalyst accumulated at the phase interface. Hence it can be concluded that TOA not only forms a complex with acetic acid, but interacts with the catalyst as well. If a

complex of TOA and acetic acid was formed and met an active site on the catalyst, it is possible that TOA bind to the catalyst instead [57], since sulfonic acid is stronger than acetic acid, and releasing acetic acid into the organic bulk. However, no change in the distribution of acetic acid was observed over time. Considering the molar ratio of TOA: catalyst (1:3, see Tab. 4-3) it was possible that TOA solely adsorbs at the catalyst, thus the observed acetic acid in the organic phase was the result of physical extraction. This assumption is supported by obtaining similar distribution of acetic acid in experiments B4 and C6. The low conversion of acetic acid might result from the occupation of active sites in both experiments. In B4 the hydration spheres hindered reaction and the active sites in C6 were occupied by TOA and hydration spheres.

No flocculation of Amberlyst® 15 was observed in one-phase experiments using TOA (experiments C1-C5). Fig. 5-4 illustrates the conversion of acetic acid with variation of the ratios of TOA: acetic acid (left diagram) and TOA: catalyst (right diagram). At 10 w% catalyst loading and no addition of TOA, a conversion of 82.2 % was achieved (C1). The addition of equimolar amounts of the amine with respect to acid showed no conversion within 180 minutes of reaction time (C5), indicating that the formed complex of amine and acetic acid is not reactive in the organic phase. The ratio of TOA: catalyst was 3:1, hence the adsorption of TOA at the active sites of Amberlyst® 15 could be an alternative explanation that no conversion was observed. A reduction of the amount of TOA to a ratio of 1:10 with respect to acetic acid and 1:3 with respect to Amberlyst® 15 resulted in a conversion of acetic acid of 16.2 % (C4). The same amount of catalyst was used as for experiments C5 and C1.

Adjusting the load of catalyst to a ratio of TOA: catalyst of 1:1 (C3) showed that conversion of acetic acid is reduced to 6 % (Fig. 5-4, right), although no conversion was expected. One explanation of observed conversion is the presence of active sites inside the catalyst pores. These pores (average diameter 300 Å, [53]) might be not accessible to the relatively bulky TOA but the smaller reactants might still diffuse into the pores and react. The same amount of catalyst and absence of the amine led to a conversion of 35.2 % (C2). The presence of TOA negatively affected the conversion of acetic acid and similar influence was observed using trialkylphospine oxides in a two-phase system [50].

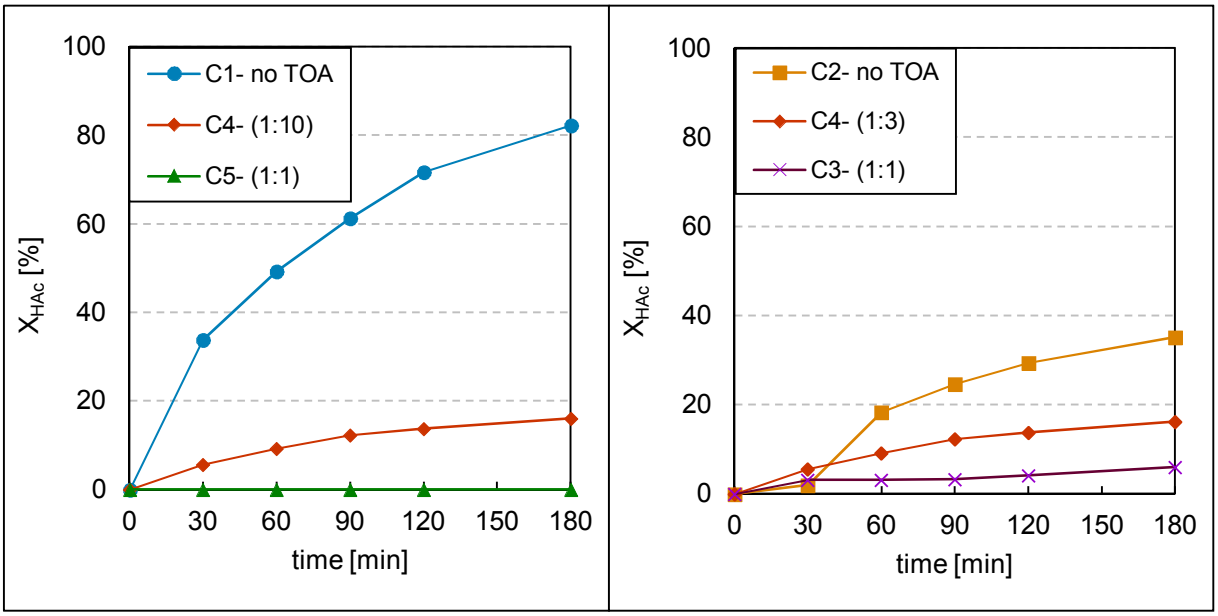


Fig. 5-4: Influence of TOA on the conversion of acetic acid in the organic phase at 50°C and ambient pressure. Numbers in paranthesis indicate the molar ratio of TOA:HAc (left) and TOA: Amberlyst® 15 (right)

The combination of reactive extraction using amines or phosphines with acid catalyzed esterification in the organic phase is not recommended due to the interaction of reactive extraction agent and catalyst. This interaction decreases the amount of reactive extraction agent available for extraction as well as the amount of active sites of the catalyst. One possibility to combine both in one intensification process is the substitution of either reactive extraction agent or catalyst with non-interacting compounds. The use of DES or inorganic solid catalyst based on metal oxides [23] might be an alternative to the acid catalyst in this context.

### 5.1.4 Physical Extraction of Acetic Acid with Variation of *n*-Octanol Mass Fraction

Fig. 5-5 (left) illustrates the density of mixtures of *n*-octanol and *n*-undecane at 50°C. A linear relationship between the density and mass fraction of *n*-octanol was observed. In contrast, the dynamic viscosity of the mixture is not strongly dependent on the mass fraction of the alcohol at lower mass fractions, but dynamic viscosity shows a linear dependence on the alcohol mass fraction with increasing concentration of *n*-octanol.

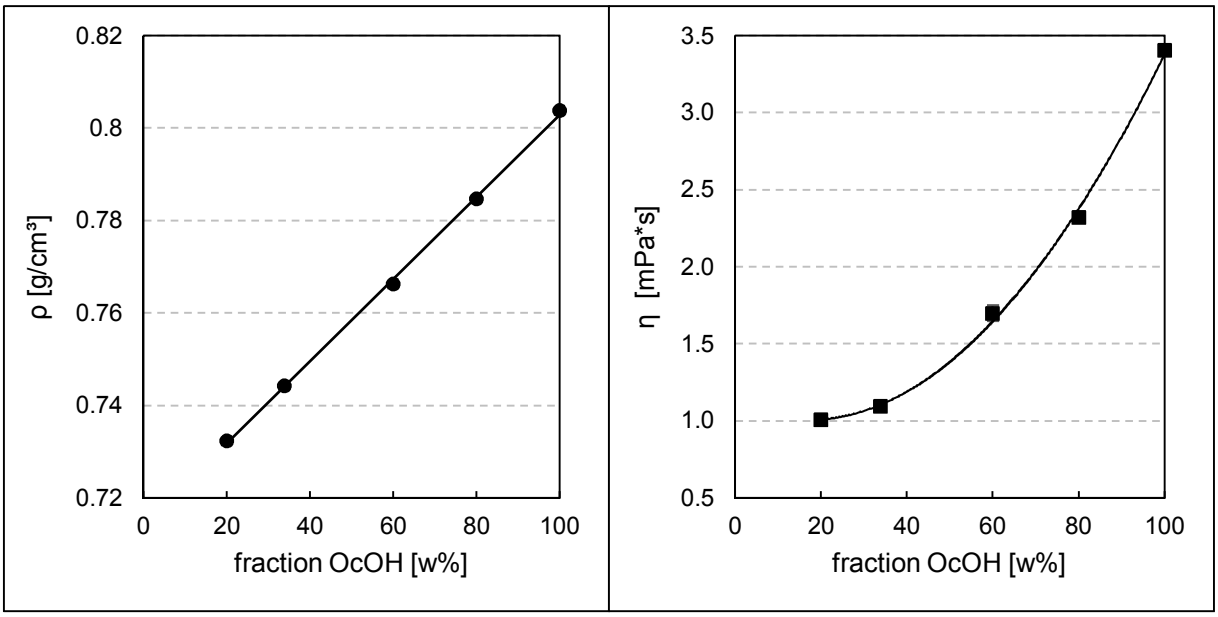


Fig. 5-5: Density (left) and dynamic viscosity (right) of mixtures of *n*-undecane and *n*- octanol at 50°C and ambient pressure

Fig. 5-6 shows the influence of *n*-octanol on the distribution of acetic acid between aqueous and organic phase at 50°C for initial 60 g/L acetic acid in the aqueous phase. The distribution was calculated by dividing the mass of acetic acid in each phase by the initial mass present in the aqueous phase. The alcohol at double molar excess with respect to acetic acid (33.8 w%) used in previous experiments (see section 5.1.1- 5.1.3) showed to extract 10 % of acetic acid into the organic phase. In case of 60 g/L acetic acid in the aqueous phase and a phase ratio of 1:1 (v/v) 6 g/L acetic acid were present in the organic phase. Pure *n*-octanol as organic phase held 25 % of the introduced acetic acid.

For subsequent use in the membrane reactor, the organic phase with 33.8 w% *n*-octanol was chosen. Advantages in form of a lower viscosity of the mixture outweigh the lower extraction capacity, if a future large scale application is considered and costs for handling the fluids depend on the density (momentum) and viscosity (friction) [58].

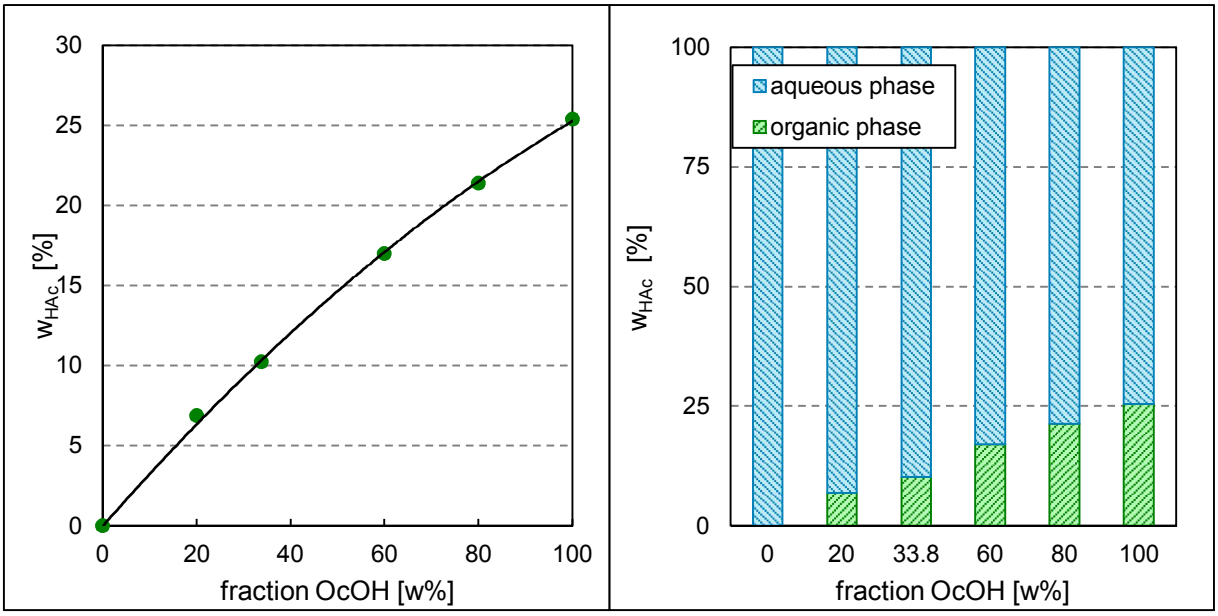


Fig. 5-6: Influence of *n*- octanol on the distribution of acetic acid between aqueous and organic phase at 50°C (right) and detailed view (left) for initial 60 g/L acetic acid in aqueous phase

## 5.2 Experiments in the Two- Phase Membrane Reactor

### 5.2.1 Homogeneous Catalysis in the Two- Phase Membrane Reactor

Tab. 5-3 summarizes the obtained critical DBSA concentrations in the small and large membrane reactor. The critical DBSA concentration is defined as the amount of DBSA in the organic phase at which no emulsion is observed in the contacting aqueous phase. The results are discussed in more detail in the following paragraphs.

Tab. 5-3: Critical DBSA concentration [in w%] in the organic phase of the small and large membrane reactor at room temperature

| | Small membrane reactor | | Large membrane reactor | |
|---|---|---|---|---|
| Membrane phase | organic | aqueous | organic | aqueous |
| Stagnant $c_{DBSA,crit}$ [w%] | 3.25[a] | N/A | 3[b] | N/A |
| Circulated $c_{DBSA,crit}$ [w%] | <1[a] | 2[a] | N/A | 1[b] |

[a] 6-7 hours, [b] 24 hours,

**Small membrane reactor with and without convection**

In the first step, the effect of the DBSA concentration on the emulsion formation was studied using the small membrane reactor and organic phase supported liquid membrane. No convection was imposed on both phases, however emulsion formation in the aqueous phase was observed and a critical DBSA concentration of $c_{DBSA,crit} = 3.25$ w% was obtained. The experiments at 3.25 w% and 3.5 w% DBSA have been repeated and critical DBSA concentration was verified. Fig. 5-7 the time until emulsion formation was observed, depending on the initial concentration of DBSA in the organic phase. The experiments were aborted after 7 hours since it was assumed that no emulsion was created after 7 hours of reaction time.

The corresponding conversion of acetic acid for the emulsion free systems is shown in Fig. 5-7 (■, right axis). The conversion was calculated by the concentration of formed octyl acetate present in the organic phase; octyl acetate was not detected in the aqueous phase as well as acetic acid was not found in the organic phase. The conversion of acetic acid remained approximately constant for experiments with $c_{DBSA} < c_{DBSA,crit}$ as indicated by the trendline.

One explanation of the similar conversions might be that the phase interface has been saturated with DBSA molecules at low concentrations already. Hence, the excess DBSA in the organic phase was not participating in the reaction which explains the similar conversion for increasing DBSA concentrations until $c_{DBSA,crit}$ was reached.

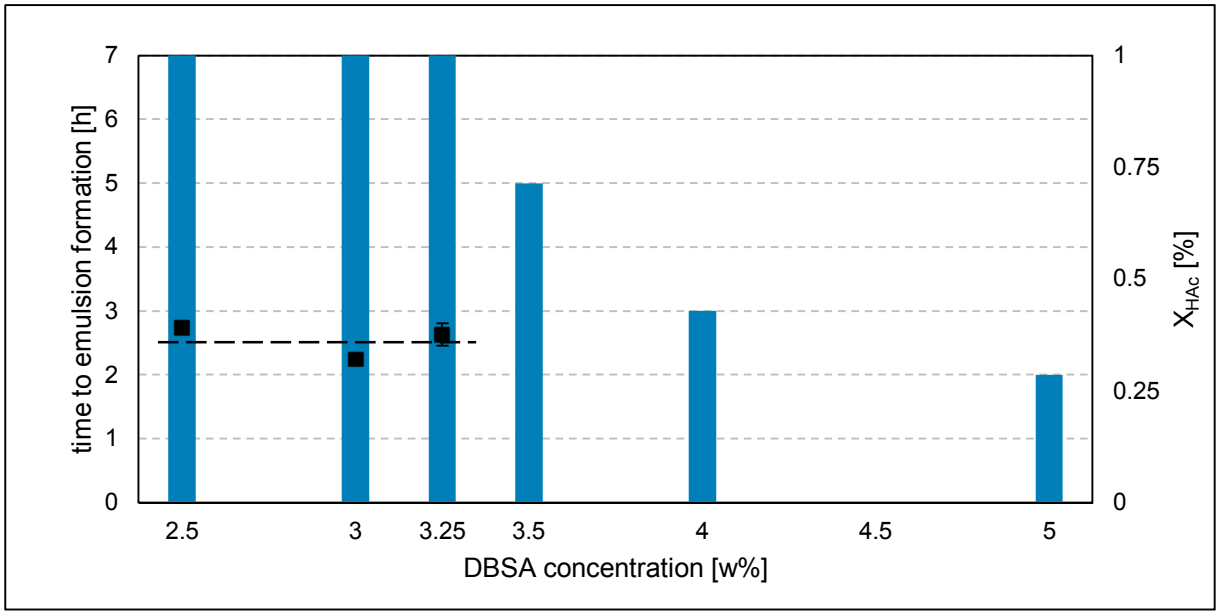


Fig. 5-7: Emulsion formation in the aqueous phase (columns, left axis) and conversion of acetic acid (■, right axis) in dependence of initial DBSA concentration in organic phase for small membrane module, stagnant phases, organic impregnated SLM at room temperature and ambient pressure

In the next step, both phases were circulated using peristaltic pumps as described in section 4.2.1. At first, the membrane was impregnated with the organic solvent and emulsion formation in the aqueous phase was observed in less than two hours for 3 w% and 1 w% DBSA in the organic phase (left diagram in Fig. 5-8). Due to the circulation, some organic phase was washed out of the liquid membrane phase. Because DBSA preferably aligned at the phase interface, more of the surfactant was introduced into the aqueous phase compared to the remaining components of the organic phase, which resulted in the formation of micelles. No emulsion was formed in the circulated organic phase. The lids on top of the membrane reactor where slightly open which allowed operation at ambient pressure and a short pressure rise due to the inlet flow of the liquid can be excluded. Hence the washing out only occurred due to the flow of the aqueous phase against the membrane phase.

Subsequently, the membrane was impregnated with the aqueous phase which ensured a stagnant aqueous zone close to the phase interface due to the rigid membrane. Fig. 5-8 (right) shows the time until emulsion in the aqueous phase was observed. Emulsion formation was not observed at DBSA concentrations below 2 w%, which supported the assumption that DBSA was washed out due to flow against the membrane phase. A conversion of acetic acid of 1.4 ± 0.2 % was obtained after 7 hours in the emulsion free systems and the trend of conversion is shown in Fig. 5-8 (right diagram) which decreases with increasing concentration of DBSA.

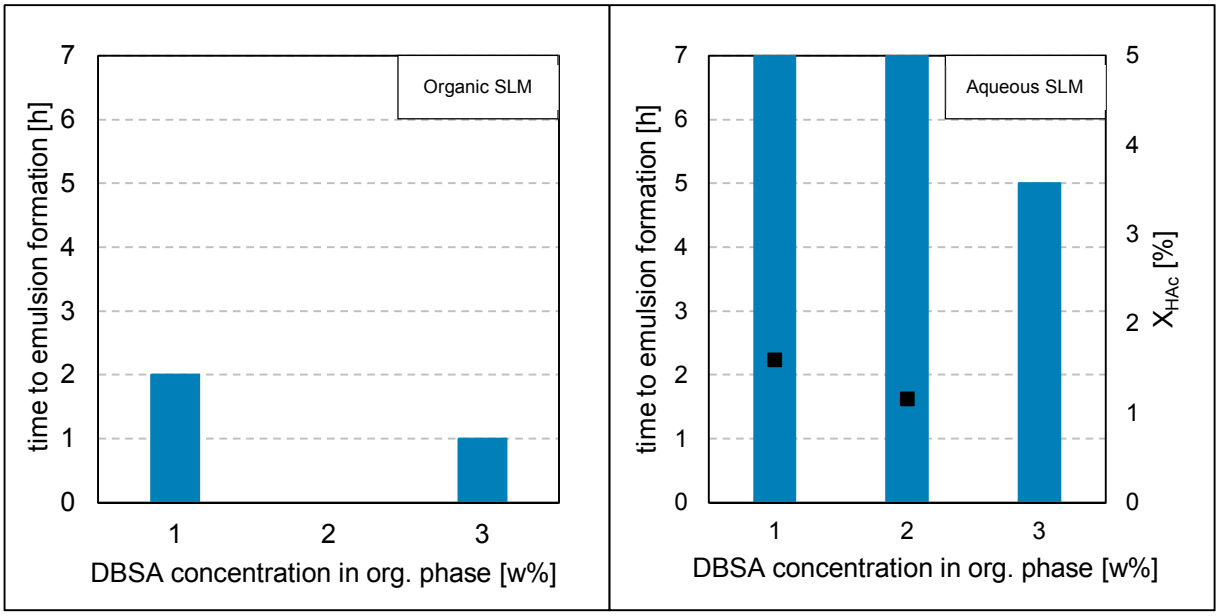


Fig. 5-8: Emulsion formation in dependence of initial DBSA concentration in organic phase for the small membrane module, circulated phases at room temperature and ambient pressure with organic phase SLM (left) and aqueous phase SLM (right) and conversion of acetic acid (■)

The formation of a separate phase on top of the aqueous phase in form of droplets (<5mm diameter) was observed in some small membrane reactor experiments with both aqueous and organic SLM. The analysis of the droplets revealed a concentration of octyl acetate of around 1.5 w% which was approximately five times the concentration found in the organic phase. In addition, around 7 w% of *n*-octanol were detected in the droplets in case of organic phase SLM. The main component in the sample was likely to be the solvent *n*-undecane since some organic phase is washed out at the filling of the reactor as some small droplets (<1mm) right

after filling indicated. Due to similar retention times of *n*-undecane and the diluents THF and *n*-heptane in the GC it was not possible to quantify the concentration of *n*-undecane.

This observation indicated that the assumed model concept developed in section 2.5 was not applicable under the performed conditions. DBSA was likely to catalyze the reaction at the phase interface as suggested at the model concept, however the resulting ester was not diffusing back into the organic phase but rather separated from the surrounding aqueous phase in form of droplets at the surface. The presence of *n*-octanol in the droplets indicates the influence of DBSA on the solubility of organic compounds in the aqueous phase.

A quantitative determination on the degree of emulsification was not possible since the sampling itself using a pipette resulted in strong emulsification of the sample and did not allow to measure optical density in a separate device. A measurement of optical density inside the reactor was not possible either, since the reactor was originally designed for a different SLM setup. Hence it could have been possible, that an emulsion was formed at DBSA concentrations where no emulsion was observed by eye. In that case, the formed micelles might have encapsulated organic compounds and released them into the aqueous phase since this mechanism is known to occur at certain concentrations of the surfactant in the aqueous phase [34].

**Large membrane reactor with and without convection**

Due to the formation of organic droplets in the aqueous phase, the phase alignment was adapted towards a horizontally oriented membrane and organic phase on top using the membrane reactor described in section 3.2.2. One experiment was performed using 3 w% DBSA and an organic impregnated membrane with stagnant phases. Within 24 hours, 3 % conversion of acetic acid was obtained and emulsion formation was not observed. No experiment was performed with the organic SLM and convection since emulsion was created in the small membrane reactor with that setup even at 1 w% DBSA.

Instead, the membrane was aqueous impregnated and the aqueous phase was circulated. Pure diffusion experiments using aqueous impregnated SLM were not performed. The flowchart of the setup is given in . A slight turbidity in aqueous phase was observed using 2 w% DBSA in the organic phase and no emulsion was recognizable at 1 w% DBSA within 24 hours of reaction time, hence $c_{DBSA,crit} = 1.0$ w%. The mean residence time $\tau$ in the large reactor was approximately half of the residence time of the small reactor. In return this resulted in a

higher velocity of the fluid in the large membrane reactor which explains emulsion formation at 2 w% where no emulsion was created at 2 w% DBSA in the small membrane reactor.

The decline of acetic acid in the aqueous phase over time for 1 w% and 2 w% DBSA is shown in Fig. 5-9. Although the measured concentrations of acetic acid for each experiment varied, a similar trend was obtained for both DBSA concentrations. At the beginning, a fast decrease of the acetic acid concentration was observed but the slope seemed to decrease with increasing time as indicated with the solid line. Compared to other esterification reactions of acetic acid [55], [59], the initial reaction rate was lower, since the reaction rate decreases with increasing alkyl chain length of the alcohol [50]. In addition, the aqueous side was only flowing through without intense mixing of the two phases and the amount of DBSA at the phase interface was not determinable. Hence a qualitative comparison of the initial reaction rates was not possible.

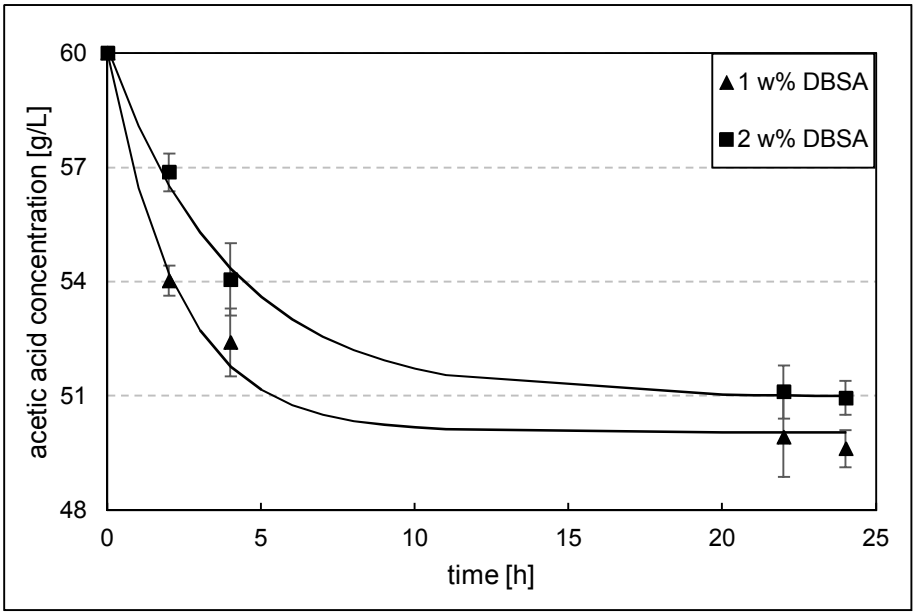


Fig. 5-9: Concentration of acetic acid over time for the large membrane reactor, circulated aqueous phase and aqueous impregnated SLM at room temperature and ambient pressure at 1 w% and 2 w% DBSA in the organic phase.

A conversion of acetic acid of 17.3 ± 0.6 % for 1 w% DBSA and 15.1 ± 0.5 % for 2 w% DBSA was obtained. The lower conversion at higher DBSA concentration might be attributed to the emulsion formation in the aqueous phase. The formed micelles in the aqueous phase close to the phase interface might have formed hydrogen bonds to the DBSA which was aligned at the phase interface. Due to the occupation of active sites by the micelles, less acetic acid reacted and migrated as octyl acetate into the organic phase. This trend of decreasing conversion with

increasing DBSA concentration was observed throughout the experiments (see Fig. 5-8) in both membrane reactors and the hypothesis of micelles occupying the active sites is one possible explanation to this observation.

### 5.2.2 Heterogeneous Catalysis in the Two- Phase Membrane Reactor

The other approach to remove acetic acid from the aqueous phase combined the physical extraction of the acid through the membrane and subsequent esterification in the organic phase. The constant conversion ensured a high concentration gradient for diffusion of acetic acid into the organic phase.

The general observed mechanism for the organic phase SLM and low concentration of acetic acid in the aqueous phase is described as follows. Due to the impregnation method, the membrane phase only contains *n*-undecane at the beginning of the experiment and acetic acid is not soluble in *n*-undecane as described in section 5.1.4. The alcohol diffuses from the organic bulk through the membrane to the phase interface and is detected in the aqueous phase approximately after 60 minutes due to the washing out (section 5.2.1). Once *n*-octanol reaches the phase interface, acetic acid will dissolve in the organic phase and diffuse into the organic bulk phase where it rapidly reacts with the catalyst, since no acetic acid is detected in the organic phase, but only octyl acetate as seen in Fig. 5-12 for 60 g/L and 120 g/L.

The effects of temperature, membrane phase and ratio of exchange area to volume ratio on the flux of acetic acid through the membrane are shown in the left diagram in Fig. 5-10. The temperature had a stronger influence on the diffusion than the A/V ratio in the investigated membrane reactors, although the flux was increased by 50 % when the A/V ratio was increased 4 times. According to Fick's Law (equation 5-2), the flux is proportional to the diffusion coefficient ($D$) and the local concentration gradient $\left(\frac{dc}{dx}\right)$ [60].

$$F = -D * \frac{dc}{dx} \tag{5-2}$$

The diffusion coefficient in liquids depends on the temperature as well as the viscosity ($\eta$) of the liquid (which in return is a function of the temperature) according to the Stokes- Einstein-Equation (equation 5-3).

$$D = \frac{k_B * T}{6 * \pi * \eta * R_0} \tag{5-3}$$

The membrane phase was impregnated with both aqueous and organic phase. Fig. 5-10 (left) shows a larger flux of acetic acid through the membrane with organic phase SLM for identical initial concentration of acetic acid in the aqueous phase of 60 g/L and 50°C temperature. The higher flux for organic phase SLM was reasoned in the lower dynamic viscosity of the organic phase (see section 5.1.4) compared to the aqueous phase which increased the diffusion coefficient according to equation 5-3.

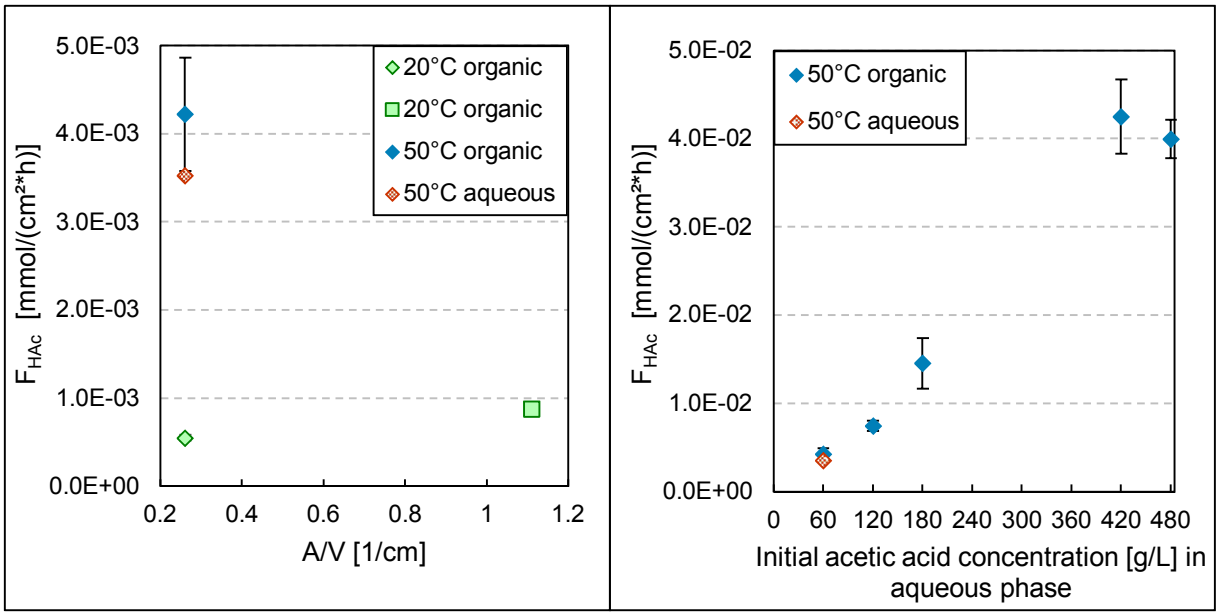


Fig. 5-10: Influence of A/V ratio, temperature, membrane phase and concentration on the flux of acetic acid. Left: small membrane reactor (◆) at 20°C and 50°C with organic and aqueous impregnated membrane and large membrane reactor (■) at 20°C at 60 g/L initial acetic acid concentration. Right: Flux of acetic acid for organic phase SLM at 50°C in the small membrane reactor in dependence on the initial acetic acid concentration in the aqueous phase

Fig. 5-10 (right) shows the dependence of the flux on the initial concentration of acetic acid in the aqueous phase. The flux was calculated by the amount of acetic acid and octyl acetate present in the organic phase divided by the reaction time and membrane area. The flux increased linearly with increasing concentration as expected according to equation 5-2. The drop in the flux at 480 g/L initial acetic acid in the aqueous phase might be explained by several observations. At high concentrations of acetic acid, emulsion formation in the aqueous phase was observed, but separated fast after the circulation of the phases was stopped. The high concentration of acetic acid increased the solubility of *n*-octanol in the aqueous phase, which in return induced the emulsion formation. The emulsion formation and dissolution of the alcohol in the aqueous phase reduced its concentration in the membrane phase, thus decreasing the

solubility of acetic acid in the organic phase and lowering the flux. At low acetic acid concentrations, almost no *n*-octanol was dissolved in the aqueous phase as Fig. 5-11 illustrates. The other, possibly more influencing factor is the aging of the membranes. The membranes have been used 50 times prior to experiments with high concentration of acetic and the alternating swelling and drying of the membrane caused visible cracks in the membrane at the edge of the membrane frame.

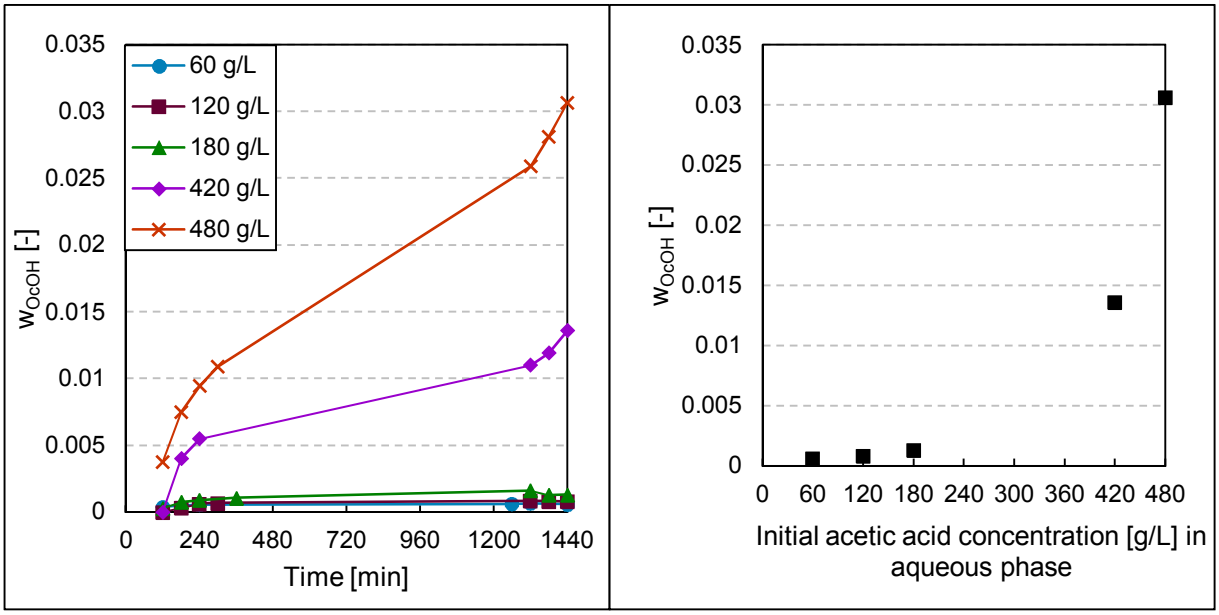


Fig. 5-11: Concentration of *n*-octanol in the aqueous phase at different acetic acid concentrations (left) and after 24 hours of reaction time (right) at 50°C and ambient pressure in the small membrane reactor

The formation of octyl acetate in the organic phase over time for different initial acetic acid concentrations in the aqueous phase is shown in the left diagram of Fig. 5-12. More product was formed with increasing concentration of acetic acid and coincides with the data of the flux of acetic acid through the membrane in Fig. 5-10 (right). At acid concentration above 120 g/L, more acetic acid diffused through the membrane than the catalyst was able to convert to octyl acetate. The amount of catalyst remained constant for all experiments on 2 w% with respect to the organic phase. Fig. 5-12 (right) shows the increase of acetic acid in the organic phase over time for the different initial acetic acid concentrations. The system at concentrations of acetic acid below 120 g/L was diffusion limited and changed to reaction limited at 180 g/L initial acid concentration. To achieve total conversion of the diffused acetic acid, the amount of cat-

alyst needs to be increased with increasing concentration of acetic acid. The higher concentration of octyl acetate at 420 g/l acetic acid than at 480 g/L correlates with the flux and the formation of emulsion in the aqueous phase.

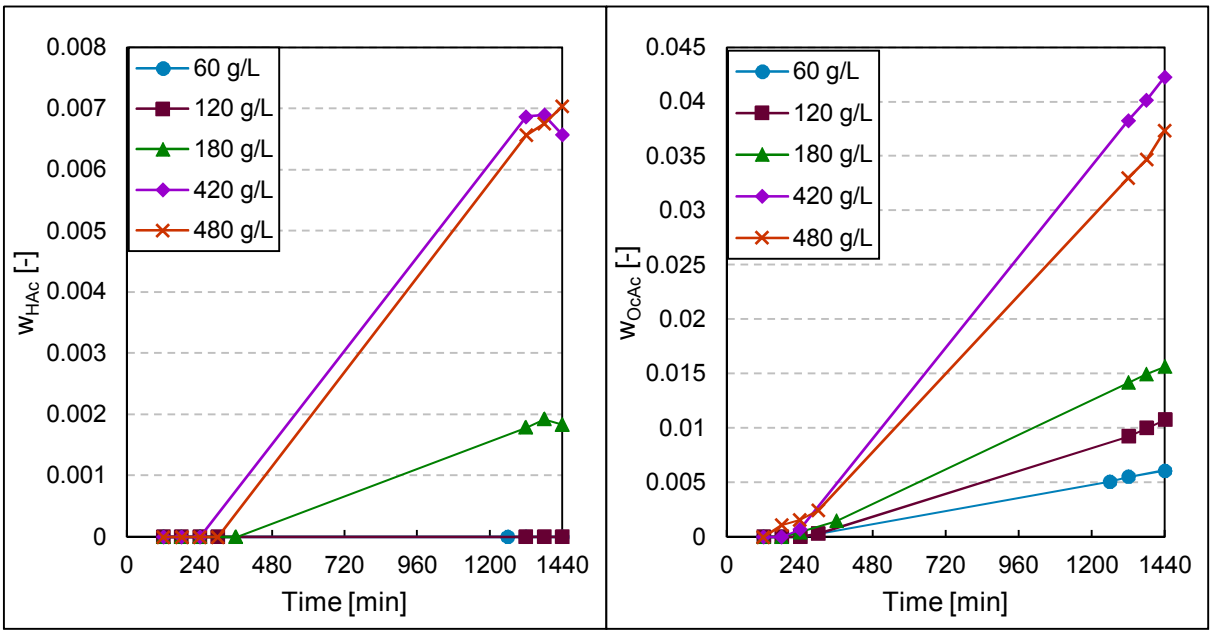


Fig. 5-12: Formation of octyl acetate (right) and increase of acetic acid (left) in the organic phase at different initial concentrations of acetic acid in the aqueous phase at 50°C and ambient pressure in the small membrane reactor

The left diagram in Fig. 5-13 shows the concentration of acetic acid and octyl acetate in the organic phase after 24 hours of reaction time in dependence of the initial acetic acid concentration. Although the total flux as well as the concentration of octyl acetate decreased from 420 g/L to 480 g/L, the concentration of acetic acid increased. All experiments were performed twice and the same trend was observed for both 480 g/L experiments. The trend might be attributed to the aforementioned aging of the membrane in combination with insufficient mixing of the organic phase and hence catalyst dispersion. The poor dispersion of the catalyst in the organic phase at low concentrations of acetic acid was not considered to affect the reaction rate since enough catalyst was added, compared to the diffused acid.

Fig. 5-13 (right) displays the conversion of acetic acid after 24 hours of reaction time in dependence on the initial acetic acid concentration. The filled rhombs consider the conversion of the acid which diffused through the membrane, the open rhombs include the conversion in the aqueous phase as well. At 420 g/L and 480 g/L initial acetic acid concentration, comparably high amounts of *n*-octanol were dissolved in the aqueous phase (Fig. 5-11), which resulted in the mentioned emulsion formation and conversion of acetic acid due to autocatalysis in the aqueous phase.

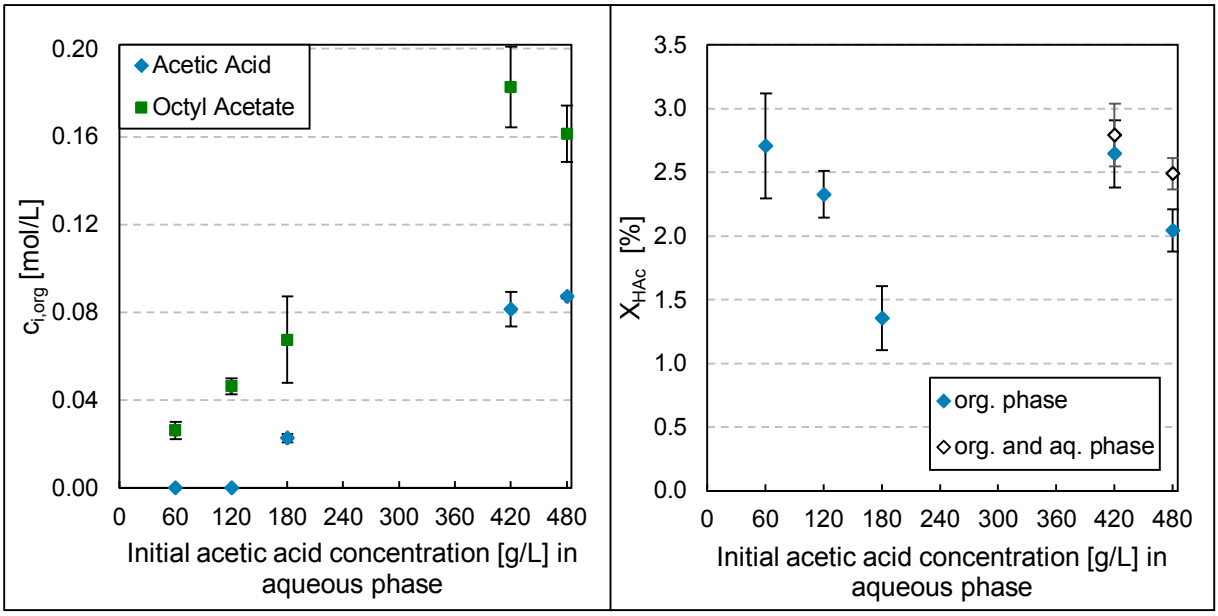


Fig. 5-13: Left: Concentration of acetic acid and octyl acetate in the organic phase after 24 hours of reaction time at 50°C in the small membrane reactor. Right: Conversion of acetic acid after 24 hours of reaction time at 50°C in the small membrane reactor depending on the initial acetic acid concentration in the aqueous phase

No emulsion was formed below 420 g/L initial acid concentration and the concentration of *n*-octanol in the organic phase remained constant over the reaction time for the experiments ≤ 180 g/L initial acetic acid (Fig. 5-11, right). Even though the concentration of octyl acetate increased with increasing initial acid concentration, the overall conversion of acetic acid decreased and was reduced by 50 % when the concentration of acetic acid was tripled. Fig. 5-13 (left) indicates, that the amount of catalyst in the organic phase was not enough to completely convert the diffused acetic acid, since the acid was detected in the organic phase, but sufficiently catalyzed the diffused acid for 60 g/L and 120 g/L acetic acid (no acetic acid was detected in the organic phase). The reason for this observation might be that a steady state in diffusion of *n*-octanol into the membrane phase was not reached during 24 hours of

reaction time. In addition, the concentration of alcohol decreased over time due to the reaction, thus less acetic acid was soluble in the organic phase. The conversion of acetic acid was below 3 % for all experiments, hence the latter reason might not be significant for the shown results, but get significant at prolonged reaction times.

Tab. 5-4 compares the conversion of acetic acid in the small (A/V = 0.26 $cm^{-1}$) and large (A/V = 1.11 $cm^{-1}$) membrane reactor at 20°C and initial 60 g/L acetic acid in the aqueous phase. No acetic acid was found in the organic phase for the small membrane reactor, but conversion of acetic acid was reduced by 87 % compared to the similar experiment at 50°C. In the large membrane reactor, the reaction rate of acetic acid at 20°C was low compared to the diffused acid. This resulted in a three times higher concentration of acetic acid than octyl acetate in the organic phase, thus showing that the conversion of acetic acid in the large membrane reactor is reaction controlled at 20°C.

Tab. 5-4: Conversion of acetic acid in the small and large membrane reactor at 20°C

| A/V [$cm^{-1}$] | $X_{HAc}$ [%] |
|---|---|
| 0.26 | 0.35 ± 0.02 |
| 1.11 | 0.55 ± 0.07 |

# 6 Summary and Conclusions

The recovery of carboxylic and hydroxycarboxylic acids in industries such as pulp and paper industry is of increasing interest due to environmental protection aspects as well as the possibility to produce a value-added product out of the waste streams [2], [4], [5]. Energy and cost intensive methods to recover the acids lead the focus on alternatives such as liquid/ liquid membrane extractions, especially for low concentrated waste streams [13], [14], [40].

Two approaches on the removal of acetic using supported liquid membrane equipment were studied. In the first approach, DBSA as a catalyst at the phase interphase was used. Direct two- phase contact in a stirred flask induced emulsification of the system even at a DBSA concentration of 0.1 w%. Due to the rigid phase interphase established by the supported liquid membrane, emulsion formation was avoided at DBSA concentrations below 1 w% in the organic phase. The energy input, characterized by the mean residence time, and nature of the liquid membrane influenced the emulsion formation and was avoided if the membrane was impregnated with aqueous phase. By changing the orientation of the membrane to horizontal phase alignment a separation of the esterification products was achieved. Octyl acetate migrated into the organic phase, whereas the side product waster remained in the aqueous phase.

The second approach combined the physical extraction of acetic acid through the liquid membrane and subsequent esterification in the organic phase catalyzed by Amberlyst® 15. The constant reaction of acetic acid with *n*-octanol in ensured the best possible concentration gradient for the diffusion of acetic acid into the organic phase. Diffusion and reaction depend on temperature. By increasing the temperature from 20°C to 50°C, the diffusion through the membrane was increased by a factor of 7.5 at acetic acid concentration of 60 g/L. An increase in the acid concentration increased flux as well, but the reaction rate limited by the amount of catalyst turned out to be the controlling factor at higher acetic acid concentrations. In addition, emulsion formation in the aqueous phase was observed at concentrations above 420 g/L acetic acid. The conversion of acetic acid increased with decreasing concentration of acetic acid in the aqueous phase, suggesting that the membrane reactor is suitable to remove carboxylic acids from diluted waste streams. To ensure a sufficient dispersion of the catalyst in one hand and decrease the volume of the organic phase on the other hand, the membrane could be functionalized with sulfonic acid groups in future experiments.

The extraction of acetic acid can be improved by increasing the concentration of *n*-octanol, but diffusion is reduced due to increasing viscosity of the organic phase. The addition of hydrogen-bond donors and reactive extraction agents such as ternary amines to enhance extraction of the acid, is not recommended since the amines interact with the solid catalyst. The utilization of a different catalyst, such as metal oxides, might reduce the interaction of the reactive extraction agent, thus facilitating a combination of reactive extraction and esterification in one phase.

Conversion of acetic acid between 2.7 % in the physical extraction experiments and 17.3 % in the phase interface- esterification within 24 hours is possible to be improved by increasing the exchange area/ volume ratio. The elevation of the temperature is limited by the boiling point of the aqueous phase and nature of the membrane. However, the operation of the membrane reactor at elevated temperatures improves the flux through the membrane, thus increasing the conversion of the extracted acetic acid.

The main advantage of the two-phase membrane reactor over the original three-phase setup is the stable membrane phase. Leaching of the membrane phase was observed in both, homogeneous and heterogeneous catalyzed experiments. The leached membrane phase was constantly renewed since the membrane phase was identical with either feed or receiving phase. The choice of membrane phase and pressure difference along the membrane allows to control the contamination of one phase with the other. For example, the contamination of the aqueous phase with organic compounds can be avoided, if the membrane phase is aqueous impregnated and a slight higher pressure is applied in that phase, ensuring that the membrane pores are filled with the aqueous phase. Thus, no subsequent phase separation is necessary.

# I. Bibliography

[1] W. Reutemann and H. Kieczka, “Formic Acid,” in *Ullmann’s Encyclopedia of Industrial Chemistry*, Weinheim, Germany: Wiley-VCH Verlag GmbH & Co. KGaA, 2014.

[2] C. Le Berre, P. Serp, P. Kalck, and G. P. Torrence, “Acetic Acid,” in *Ullmann’s Encyclopedia of Industrial Chemistry*, Weinheim, Germany: Wiley-VCH Verlag GmbH & Co. KGaA, 2014.

[3] J. N. Starr and G. Westhoff, “Lactic Acid,” in *Ullmann’s Encyclopedia of Industrial Chemistry*, Weinheim, Germany: Wiley-VCH Verlag GmbH & Co. KGaA, 2014.

[4] M. Hundt, “Der AlkaPolP-Prozess als Ausgangspunkt für eine lignocellulosebasierte Bioraffinerie,” Brandenburgischen Technischen Universität Cottbus-Senftenberg, 2015.

[5] E. Sjoestroem, “The behavior of wood polysaccharides during alkaline pulping processes,” *Tappi J.*, vol. 60, no. 9, pp. 151–154, 1977.

[6] B. Saha, “Recovery of dilute acetic acid through esterification in a reactive distillation column,” *Catal. Today*, vol. 60, no. 1–2, pp. 147–157, Jul. 2000.

[7] A. Arpornwichanop, K. Koomsup, and S. Assabumrungrat, “Hybrid reactive distillation systems for n-butyl acetate production from dilute acetic acid,” *J. Ind. Eng. Chem.*, vol. 14, no. 6, pp. 796–803, Nov. 2008.

[8] V. D. Talnikar and Y. S. Mahajan, “Recovery of acids from dilute streams : A review of process technologies,” *Korean J. Chem. Eng.*, vol. 31, no. 10, pp. 1720–1731, Aug. 2014.

[9] B. Reddy, R. Bhat, A. Agrawal, P. Patidar, and S. Mahajani, “Comparison of reactive chromatography and reactive distillation for the synthesis of C1–C4 acetates,” *Chem. Eng. Process. Process Intensif.*, vol. 95, pp. 17–25, Sep. 2015.

[10] M. Henczka and M. Djas, “Reactive extraction of acetic acid and propionic acid using supercritical carbon dioxide,” *J. Supercrit. Fluids*, vol. 110, pp. 154–160, Apr. 2016.

[11] A. Arpornwichanop, K. Koomsup, W. Kiatkittipong, P. Praserthdam, and S. Assabumrungrat, “Production of n-butyl acetate from dilute acetic acid and n-butanol using different reactive distillation systems: Economic analysis,” *J. Taiwan Inst. Chem. Eng.*, vol. 40, no. 1, pp. 21–28, Jan. 2009.

[12] G. Yang, M. S. Jahan, L. Ahsan, L. Zheng, and Y. Ni, “Recovery of acetic acid from pre-hydrolysis liquor of hardwood kraft-based dissolving pulp production process by reactive extraction with triisooctylamine.,” *Bioresour. Technol.*, vol. 138, pp. 253–8, Jun. 2013.

[13] Š. Schlosser, R. Kertész, and J. Marták, “Recovery and separation of organic acids by membrane-based solvent extraction and pertraction: An overview with a case study on

recovery of MPCA," *Sep. Purif. Technol.*, vol. 41, no. 3, pp. 237–266, 2005.

[14] D. L. Grzenia, R. W. Dong, H. Jasuja, M. J. Kipper, X. Qian, and S. Ranil Wickramasinghe, "Conditioning biomass hydrolysates by membrane extraction," *J. Memb. Sci.*, vol. 415, pp. 75–84, 2012.

[15] T. Teerachaiyapat and P. Ramakul, "Application of hollow fiber supported liquid membrane as a chemical reactor for esterification of lactic acid and ethanol to ethyl lactate," *Korean J. Chem. Eng.*, vol. 33, no. 1, pp. 8–13, Dec. 2015.

[16] A. Alegría, Á. L. F. de Arriba, J. R. Morán, and J. Cuellar, "Biodiesel production using 4-dodecylbenzenesulfonic acid as catalyst," *Appl. Catal. B Environ.*, vol. 160, pp. 743–756, 2014.

[17] A. Alegría and J. Cuellar, "Esterification of oleic acid for biodiesel production catalyzed by 4-dodecylbenzenesulfonic acid," *Appl. Catal. B Environ.*, vol. 179, pp. 530–541, 2015.

[18] T. Dittmar, T. Dimmig, B. Ondruschka, B. Heyn, J. Haupt, and M. Lauterbach, "Herstellung von Fettsäuremethylestern aus Rapsöl und Altfetten im diskontinuierlichen Betrieb," *Chemie Ing. Tech.*, vol. 75, no. 5, pp. 595–601, May 2003.

[19] A. M. AL Sabagh, N. E. Maysour, and M. R. Noor El Din, "Investigate the Demulsification Efficiency of Some Novel Demulsifiers in Relation to Their Surface Active Properties," *J. Dispers. Sci. Technol.*, vol. 28, no. 4, pp. 547–555, Apr. 2007.

[20] J. Sjöblom, *Encyclopedic handbook of emulsion technology*. Marcel Dekker, 2001.

[21] J. Draxler and R. Marr, "Auslegungskriterien für elektrostatische Emulsionsspaltanlagen," *Chemie Ing. Tech.*, vol. 62, no. 7, pp. 523–530, 1990.

[22] J. Liu, P. Li, L. Chen, Y. Feng, W. He, and X. Lv, "Modified superhydrophilic and underwater superoleophobic PVDF membrane with ultralow oil-adhesion for highly efficient oil/water emulsion separation," 2016.

[23] J. Otera and J. Nishikido, *Esterification: methods, reactions and applications*, 2nd ed. Weinheim, Germany: Wiley-VCH Verlag GmbH & Co. KGaA, 2010.

[24] O. Levenspiel, *Chemical Reaction Engineering*, 3rd ed. New York: John Wiley & Sons, 1999.

[25] Y. P. Bruice, *Organic Chemistry*, 7th ed. Pearson Education, Inc, 2014.

[26] G. Genduso, P. Luis, and B. Van der Bruggen, "Pervaporation membrane reactors (PVMRs) for esterification," in *Membrane Reactors for Energy Applications and Basic Chemical Production*, 1st ed., vol. 1, Elsevier Ltd, 2015, pp. 565–603.

[27] M. Vafaeezadeh and A. Fattahi, "DFT investigations for 'Fischer' esterification mechanism over

silica-propyl-SO3H catalyst: Is the reaction reversible?," *Comput. Theor. Chem.*, vol. 1071, pp. 27–32, Nov. 2015.

[28] S. Miao and B. H. Shanks, "Mechanism of acetic acid esterification over sulfonic acid-functionalized mesoporous silica," *J. Catal.*, vol. 279, no. 1, pp. 136–143, Apr. 2011.

[29] Y. Liu, E. Lotero, and J. G. Goodwin, "A comparison of the esterification of acetic acid with methanol using heterogeneous versus homogeneous acid catalysis," *J. Catal.*, vol. 242, no. 2, pp. 278–286, 2006.

[30] S. M. Hashmi, K. X. Zhong, and A. Firoozabadi, "Acid–base chemistry enables reversible colloid-to-solution transition of asphaltenes in non-polar systems," *Soft Matter*, vol. 8, no. 33, p. 8778, 2012.

[31] S. Khandelwal, Y. K. Tailor, and M. Kumar, "Deep eutectic solvents (DESs) as eco-friendly and sustainable solvent/catalyst systems in organic transformations," *J. Mol. Liq.*, vol. 215, pp. 345–386, Mar. 2016.

[32] V. De Santi, F. Cardellini, L. Brinchi, and R. Germani, "Novel Brønsted acidic deep eutectic solvent as reaction media for esterification of carboxylic acid with alcohols," *Tetrahedron Lett.*, vol. 53, no. 38, pp. 5151–5155, Sep. 2012.

[33] T. F. Tadros, *Emulsions*. Berlin, Boston: De Gruyter, 2016.

[34] H. Mollet and A. Grubenmann, *Formulierungstechnik*. Weinheim, Germany: WILEY-VCH Verlag GmbH & Co. KGaA, 1999.

[35] K. Peter, C. Vollhardt, and E. Schore, *Organische Chemie*. Berlin, Heidelberg: Springer Berlin Heidelberg, 2011.

[36] P. C. Wankat, "Liquid- Liquid Extraction," in *Separation process engineering*, 3rd ed., Prentice Hall, 2012, pp. 507–508.

[37] H.-J. Bart, *Reactive Extraction*. Springer Berlin Heidelberg, 2001.

[38] A. Keshav, K. L. Wasewar, S. Chand, and H. Uslu, "Effect of binary extractants and modifier–diluents systems on equilbria of propionic acid extraction," *Fluid Phase Equilib.*, vol. 275, no. 1, pp. 21–26, 2009.

[39] M. E. Marti, "Solvent modification effect on the physical and chemical extraction of acetic acid," *Sep. Sci. Technol.*, vol. 51, no. 11, pp. 1806–1816, Jul. 2016.

[40] D. L. Grzenia, D. J. Schell, and S. R. Wickramasinghe, "Membrane extraction for removal of acetic acid from biomass hydrolysates," *J. Memb. Sci.*, vol. 322, no. 1, pp. 189–195, Sep. 2008.

[41] R. A. Bartsch and J. D. Way, “Chemical Separations with Liquid Membranes: An Overview,” in *ACS Symposium Series 642*, 1996, pp. 1–10.

[42] V. S. Kislik, “Chapter 1- Introduction, General Description, Definitions, and Classification. Overview,” in *Liquid Membranes*, Elsevier, 2010, pp. 1–15.

[43] P. Dżygiel and P. P. Wieczorek, “Chapter 3- Supported Liquid Membranes and Their Modifications: Definition, Classification, Theory, Stability, Application and Perspectives,” in *Liquid Membranes*, Elsevier, 2010, pp. 73–140.

[44] S. Retschitzegger, “Kontinuierlicher Betrieb einer Versuchsanlage für die Flüssigmembranpermeation mit gestützten Membranen,” Technische Universität Graz, 2012.

[45] H. Leopold and H. Stabinger, “Vorrichtung zur Bestimmung der Dichte von Flüssigkeiten und Gasen aus der Periodendauer eines mit einem Präparat gefüllten Messschwingers,” AT 399051 B, 1992.

[46] “Stabinger Viskosimeter SVM 3000.” [Online]. Available: http://www.anton-paar.com/?eID=documentsDownload&document=53279&L=2. [Accessed: 06-Oct-2016].

[47] G. Hradetzky, “Moderne Präzisionsdichtemessung für Flüssigkeiten,” *Mitteilungsblatt d. Chem. Ges. d. DDR*, vol. 30, pp. 162–166, 1983.

[48] C. F. Poole and L. M. Blumberg, “Chapter 2 – Theory of Gas Chromatography,” in *Gas Chromatography*, 2012, pp. 19–78.

[49] C. F. Poole and M. S. Klee, “Chapter 12 – Detectors,” in *Gas Chromatography*, 2012, pp. 307–347.

[50] A. Toth, “Intensivierung der Carbonsäureisolierung aus wässrigen Prozessströmen durch kombinierte Extraktion und Veresterung,” Technische Universität Graz, 2015.

[51] V. Ragaini, C. L. Bianchi, C. Pirola, and G. Carvoli, “Increasing the value of dilute acetic acid streams through esterification,” *Appl. Catal. B Environ.*, vol. 64, no. 1–2, pp. 66–71, Apr. 2006.

[52] GESTIS-Stoffdatenbank, “Institut für Arbeitsschutz der Deutschen Gesetzlichen Unfallversicherung.” [Online]. Available: http://gestis.itrust.de. [Accessed: 28-Nov-2016].

[53] The Dow Chemical Company, “Product Search Dow Chemcical Company.” [Online]. Available: http://www.dow.com/assets/attachments/business/process_chemicals/amberlyst/amberlyst_15wet/tds/amberlyst_15wet.pdf. [Accessed: 30-Nov-2016].

[54] J. Lilja, D. Y. Murzin, T. Salmi, J. Aumo, P. Ma??ki-Arvela, and M. Sundell, “Esterification of different acids over heterogeneous and homogeneous catalysts and correlation with the taft equation,” *J. Mol. Catal. A Chem.*, vol. 182, no. 183, pp. 555–563, 2002.

[55] Y. Liu, E. Lotero, and J. G. Goodwin, “Effect of water on sulfuric acid catalyzed esterification,” *J. Mol. Catal. A Chem.*, vol. 245, no. 1–2, pp. 132–140, Feb. 2006.

[56] H. Müller, “Sulfuric Acid and Sulfur Trioxide,” in *Ullmann’s Encyclopedia of Industrial Chemistry*, Weinheim, Germany: Wiley-VCH Verlag GmbH & Co. KGaA, 2014.

[57] D. L. Grzenia, D. J. Schell, and S. Ranil Wickramasinghe, “Membrane extraction for detoxification of biomass hydrolysates,” *Bioresour. Technol.*, vol. 111, pp. 248–254, 2012.

[58] P. B. Meherwan, “Transport and Storage of Fluids,” in *Perry’s Chemical Engineers’ Handbook*, 8th ed., McGraw-Hill, 2008.

[59] M. Mekala and V. R. Goli, “Kinetics of esterification of methanol and acetic acid with mineral homogeneous acid catalyst,” *Chinese J. Chem. Eng.*, vol. 23, no. 1, pp. 100–105, Jan. 2015.

[60] E. L. Cussler, *Diffusion: mass transfer in fluid systems*, 3rd ed. Cambridge: Cambridge University Press, 2009.

# II. List of Figures

# III. List of Tables

# IV. List of Abbreviations

General Symbols

| | |
|---|---|
| BLM | Bulk liquid membrane |
| D2EHPA | Di(2-ethylhexyl) phosphoric acid |
| DBSA | *4*-dodecylbenzenesulfonic acid |
| CMC | Critical micelle concentration |
| DES | Deep eutectic solvent |
| DFT | Density functional theory |
| ELM | Emulsion liquid membrane |
| FID | Flame ionization detector |
| GC | Gas chromatograph |
| HAc | Acetic acid |
| IL | Ionic Liquid |
| ILM | Immobilized liquid membrane |
| OcAc | Octyl acetate |
| OcOH | *n*-octanol |
| PTFE | Polytetrafluoroethylene |
| PTSA | *p*- Toluenesulfonic acid monohydrate |
| PVC-U | Polyvinylchloride – rigid |
| SLM | Supported liquid membrane |
| TCyAMsO | Trimethylcyclohexyl ammonium methanesolfonate |
| THF | Tetrahydrofuran |
| TOA | Trioctylamine |
| UNF | Unified thread standard - fine |

Formular Symbols

| Symbol | Unit | Description |
|---|---|---|
| $Area_i$ | $[pA * min]$ | Peak area of compound $i$ in sample |
| $A_{in}$ | $[m^2]$ | Cross sectional area of inlet |
| $A_{new}$ | $[m^2]$ | New surface area created |
| $c_{DBSA,crit}$ | $[w\%]$ | Critical concentration of DBSA in the organic phase |
| $D$ | $\left[\frac{m^2}{sec}\right]$ | Diffusion coefficient |
| $E_{in}$ | $[J]$ | Energy input into system |
| $F$ | $\left[\frac{mol}{m^2 * sec}\right]$ | Flux of a substance due to diffusion |
| $f_{c,i}$ | $\left[\frac{w_i}{A}\right]$ | Calibration factor of compound $i$ for gas chromatography |
| $F_c$ | $[N]$ | Force needed to compensate imbalanced surface interaction |
| $f_d$ | $\left[\frac{g}{g}\right]$ | Dilution factor of sample |
| $k_B$ | $\left[\frac{J}{K}\right]$ | Boltzmann constant |
| $K_{D\,i}$ | $[-]$ | Distribution coefficient of compound $i$ |
| $l$ | $[m]$ | Unit length at which $F$ is acting parallel to surface |
| $m_{diluted\ \ sample}$ | $[g]$ | Mass of diluted sample |
| $m_{empty\ \ vial}$ | $[g]$ | Mass of empty vial |
| $m_i$ | $[g]$ | Mass of substance $i$ |
| $m_{sample+vial}$ | $[g]$ | Total mass of sample and vial |
| $m_{total}$ | $[g]$ | Total mass of mixture |
| $n_{HAc,0}$ | $[mol]$ | Initial amount of acetic acid in system |
| $n_{HAc,t}$ | $[mol]$ | Amount of acetic acid in system at time $t$ |
| $n_{OcAc,t}$ | $[mol]$ | Amount of octyl acetate in system at time $t$ |
| $R_0$ | $[m]$ | Radius of diffusion particle |
| $V$ | $[ml]$ | Reactor volume |
| $\dot{V}$ | $\left[\frac{ml}{min}\right]$ | Pump flow rate |
| $v$ | $\left[\frac{m}{sec}\right]$ | Inlet velocity |
| $w_i$ | $\left[\frac{g}{g}\right]$ | Weight fraction of compound $i$ |

| | | |
|---|---|---|
| $X_{HAc,t}$ | $[\%]$ | Conversion of acetic acid at time $t$ |
| $\Delta G_{surf}$ | $\left[\frac{J}{m^2}\right]$ | Free surface energy |
| $\tau$ | $[min]$ | Mean residence time |
| $\eta$ | $[Pa * s]$ | Dynamic viscosity |
| $\sigma_{surf}$ | $\left[\frac{N}{m}\right]$ | Surface tension |
| $\frac{dc}{dx}$ | $\left[\frac{mol}{m^4}\right]$ | Local concentration gradient |

# V. Specification of Gas Chromatography and Used Chemicals

Tab. 6-1: Specification of gas chromatography

| | |
|---|---|
| Device | Agilent 6890N |
| Column | Agilent VF-WAXms (60 x 0.25 x 0.5) |
| Injection temperature | 250°C |
| Detector | Flame ionization detector at 280°C |
| Method | 80°C for 1 minute<br>Rate 5°C/minute until 200°C |

Tab. 6-2: Used chemicals

| | CAS-No. | MW [g/mol] | ρ[a] [g/cm³] | Use | Vendor | Purity |
|---|---|---|---|---|---|---|
| Acetic acid | 64-19-7 | 60.1 | 1.05 | Reactant | Sigma Aldrich | 99-100 % |
| 4- Dodecylbenzenesulfonic acid | 121-65-3 | 326.5 | 1.2 | Catalyst | Sigma Aldrich | ≥ 95 % |
| p- Toluenesulfonic acid monohydrate | 6192-52-5 | 190.2 | N/A | Precursor DES | Sigma Aldrich | ≥ 98.5 % |
| N,N- Dimethylcyclohexylamine | 98-94-2 | 127.2 | 0.85[b] | Precursor DES | Sigma Aldrich | 99 % |
| Methyl methansulfonate | 66-27-3 | 110.1 | 1.3[b] | Precursor DES | Sigma Aldrich | 99 % |
| n-Octanol | 111-87-5 | 130.2 | 0.82 | Reactant | Sigma Aldrich | ≥ 98 % |
| n-Heptane | 142-82-5 | 100.2 | 0.68 | Solvent | Sigma Aldrich | ≥ 99 % |
| n-Undecane | 1120-21-4 | 156.3 | 0.74 | Solvent | Sigma Aldrich | ≥ 95 % |
| Octyl acetate | 112-14-1 | 172.3 | 0.87 | Product | Sigma Aldrich | ≥ 99 % |
| Amberlyst® 15 | 39389-20-3 | N/A | N/A | Catalyst | Sigma Aldrich | dry |
| Trioctylamine | 1116-76-3 | 353.7 | 0.81 | Reactive Extractant | Acros Organics | 97 % |

[a] at 20°C unless otherwise indicated, [b] at 25°C

# VI. Supplementary data of presented figures

Fig 5-2
Amberlyst 15

| time | $X_{HAc}$ | $w_{HAc,aq}$ | $w_{HAc,org}$ |
|---|---|---|---|
| [min] | [%] | [%] | [%] |
| 0 | 0.00 | 100.00 | 0.00 |
| 30 | 0.00 | 87.58 | 12.42 |
| 60 | 0.00 | 87.50 | 12.50 |
| 90 | 0.00 | 85.01 | 14.99 |
| 120 | 0.00 | 85.28 | 14.72 |
| 180 | 0.19 | 88.20 | 11.80 |

Sulfuric acid

| time | $X_{HAc}$ | $w_{HAc,aq}$ | $w_{HAc,org}$ |
|---|---|---|---|
| [min] | [%] | [%] | [%] |
| 0 | 0.00 | 100.00 | 0.00 |
| 30 | 0.63 | 89.56 | 10.44 |
| 60 | 0.64 | 92.81 | 7.19 |
| 120 | 0.72 | 93.51 | 6.49 |
| 180 | 0.78 | 94.35 | 5.65 |

Fig 5-3
Amberlyst 15

| time | $X_{HAc}$ | $w_{HAc,aq}$ | $w_{HAc,org}$ |
|---|---|---|---|
| [min] | [%] | [%] | [%] |
| 0 | 0.00 | 100.00 | 0.00 |
| 30 | 0.00 | 83.10 | 16.90 |
| 60 | 0.00 | 84.24 | 15.76 |
| 90 | 0.00 | 84.23 | 15.77 |
| 120 | 0.00 | 84.40 | 15.60 |
| 180 | 0.21 | 83.79 | 16.21 |

Fig 5-4

| time | $X_{HAc}$ [%] | | | | |
|---|---|---|---|---|---|
| [min] | C1 | C2 | C3 | C4 | C5 |
| 0 | 0.00 | 0.00 | 0.00 | 0.00 | 0.00 |
| 30 | 33.80 | 1.95 | 3.16 | 5.61 | 0.00 |
| 60 | 49.27 | 18.33 | 3.12 | 9.22 | 0.00 |
| 90 | 61.37 | 24.71 | 3.33 | 12.37 | 0.00 |
| 120 | 71.69 | 29.41 | 4.09 | 13.72 | 0.00 |
| 180 | 82.21 | 35.20 | 6.04 | 16.15 | 0.00 |

Fig 5-5

| | Density | | Dynamic viscosity | |
|---|---|---|---|---|
| $w_{OcOH}$ | Mean | Std | Mean | Std |
| [%] | [g/cm³] | [g/cm³] | [g/cm³] | [g/cm³] |
| 20 | 0.7324 | 0.00E+00 | 1.0081 | 1.50E-03 |
| 33.8 | 0.7442 | 0.00E+00 | 1.0942 | 5.00E-05 |
| 60 | 0.7663 | 5.00E-05 | 1.6988 | 5.36E-02 |
| 80 | 0.7847 | 5.00E-05 | 2.3207 | 1.00E-04 |
| 100 | 0.8039 | 5.00E-05 | 3.4041 | 8.25E-03 |

Fig 5-6

| $w_{OcOH}$ [%] | $w_{HAc,aq}$ Mean [%] | $w_{HAc,org}$ Mean [%] | Std [%] |
|---|---|---|---|
| 0 | 100.00 | 0.00 | 0.00 |
| 20 | 93.13 | 6.87 | 0.08 |
| 33.8 | 89.77 | 10.23 | 0.04 |
| 60 | 83.02 | 16.98 | 0.09 |
| 80 | 78.63 | 21.37 | 0.02 |
| 100 | 74.60 | 25.40 | 0.09 |

Fig 5-7

| $w_{DBSA}$ [%] | $X_{HAc}$ [%] | Std [%] |
|---|---|---|
| 2.5 | 0.39 | - |
| 3 | 0.32 | - |
| 3.25 | 0.375 | 0.025 |

Fig 5-8

| $w_{DBSA}$ [%] | $X_{HAc}$ [%] |
|---|---|
| 1 | 1.6 |
| 2 | 1.17 |

Fig 5-9

| time | 2 w% DBSA $c_{HAc}$ | 2 w% DBSA Std | 1 w% DBSA $c_{HAc}$ | 1 w% DBSA Std |
|---|---|---|---|---|
| [h] | [g/L] | [g/L] | [g/L] | [g/L] |
| 0 | 60.00 | - | 60.00 | - |
| 2 | 56.87 | 0.50 | 54.02 | 0.39 |
| 4 | 54.05 | 0.95 | 52.39 | 0.89 |
| 22 | 51.10 | 0.70 | 49.91 | 1.05 |
| 24 | 50.94 | 0.45 | 49.61 | 0.49 |

Fig 5-10 left

| A/V [$cm^{-1}$] | T [°C] | $F_{HAc}$ [mmol/(cm²*h)] | Phase [-] |
|---|---|---|---|
| 0.26 | 50 | 0.0042 | organic |
| 0.26 | 50 | 0.0035 | aqueous |
| 0.26 | 20 | 0.0005 | organic |
| 1.11 | 20 | 0.0009 | organic |

Fig 5-10 right

| $c_{HAc}$ [g/L] | $F_{HAc}$ [mmol/(cm²*h)] | Phase [-] |
|---|---|---|
| 60 | 0.0042 | organic |
| 120 | 0.0075 | organic |
| 180 | 0.0145 | organic |
| 420 | 0.0425 | organic |
| 480 | 0.0400 | organic |
| 60 | 0.0035 | aqueous |

Fig 5-11 left and right (entry at 1440 min)

| time | $w_{OcOH}$ [-] initial acetic acid concentration | | | | |
|---|---|---|---|---|---|
| [min] | 60 g/L | 120 g/L | 180 g/L | 420 g/L | 480 g/L |
| 120 | 0.0004 | 0.0000 | 0.0003 | 0.0000 | 0.0038 |
| 180 | 0.0006 | 0.0003 | 0.0008 | 0.0040 | 0.0075 |
| 240 | | 0.0006 | 0.0009 | 0.0055 | 0.0095 |
| 300 | | 0.0007 | | | 0.0109 |
| 360 | | | 0.0011 | | |
| 1260 | 0.0006 | | | | |
| 1320 | 0.0006 | 0.0008 | 0.0016 | 0.0110 | 0.0259 |
| 1380 | | 0.0008 | 0.0013 | 0.0119 | 0.0281 |
| 1440 | 0.0006 | 0.0008 | 0.0013 | 0.0136 | 0.0307 |

Fig 5-12 left

$w_{HAc}$ [-]

| time | initial acetic acid concentration | | | | |
|---|---|---|---|---|---|
| [min] | 60 g/L | 120 g/L | 180 g/L | 420 g/L | 480 g/L |
| 120 | 0 | 0 | 0 | 0 | 0 |
| 180 | 0 | 0 | 0 | 0 | 0 |
| 240 | | 0 | 0 | 0 | 0 |
| 300 | | 0 | | | 0 |
| 360 | | | 0 | | |
| 1260 | 0 | | | | |
| 1320 | 0 | 0 | 0.0018 | 0.0069 | 0.0066 |
| 1380 | | 0 | 0.0019 | 0.0069 | 0.0068 |
| 1440 | 0 | 0 | 0.0018 | 0.0066 | 0.0070 |

Fig 5-12 right

$w_{OcAc}$ [-]

| time | initial acetic acid concentration | | | | |
|---|---|---|---|---|---|
| [min] | 60 g/L | 120 g/L | 180 g/L | 420 g/L | 480 g/L |
| 120 | 0 | 0 | 0 | 0 | 0 |
| 180 | 0 | 0 | 0 | 0 | 0.0011 |
| 240 | | 0 | 0.0004 | 0.0007 | 0.0016 |
| 300 | | 0.0003 | | | 0.0025 |
| 360 | | | 0.0015 | | |
| 1260 | 0.0051 | | | | |
| 1320 | 0.0055 | 0.0092 | 0.0142 | 0.0383 | 0.0330 |
| 1380 | | 0.0100 | 0.0150 | 0.0402 | 0.0347 |
| 1440 | 0.0061 | 0.0107 | 0.0156 | 0.0423 | 0.0373 |

Fig 5-13 left

| Init $c_{HAc}$ [g/L] | $c_{HAc}$ [g/mol] | $c_{OcAc}$ [g/mol] |
|---|---|---|
| 60 | 0 | 0.026 |
| 120 | 0 | 0.046 |
| 180 | 0.023 | 0.068 |
| 420 | 0.081 | 0.183 |
| 480 | 0.087 | 0.161 |

Fig 5-13 right

| | $X_{HAc}$ [%] | |
|---|---|---|
| Init. $c_{HAc}$ [g/L] | organic phase | org and aqu. phase |
| 60 | 2.70 | |
| 120 | 2.33 | |
| 180 | 1.36 | |
| 420 | 2.65 | 2.79 |
| 480 | 2.05 | 2.49 |